การพัฒนาเทคนิคสำหรับการคัดกรองของเหลวในภาชนะปิดโดยใช้การทะลุผ่านของรังสีเอกซ์พลังงานต่ำ

นายภาคภูมิ อรชร

วิทยานิพนธ์นี้เป็นส่วนหนึ่งของการศึกษาตามหลักสูตรปริญญาวิศวกรรมศาสตรดุษฎีบัณฑิต
สาขาวิชาวิศวกรรมนิวเคลียร์ ภาควิชาวิศวกรรมนิวเคลียร์
คณะวิศวกรรมศาสตร์ จุฬาลงกรณ์มหาวิทยาลัย
ปีการศึกษา 2560
ลิขสิทธิ์ของจุฬาลงกรณ์มหาวิทยาลัย

DEVELOPMENT OF TECHNIQUE FOR SCREENING LIQUIDS IN UNOPENED BOTTLE USING L
OW ENERGY X-RAY TRANSMISSION

Mr. Parkphum Orachorn

จุฬาลงกรณ์มหาวิทยาลัย
CHULALONGKORN UNIVERSITY
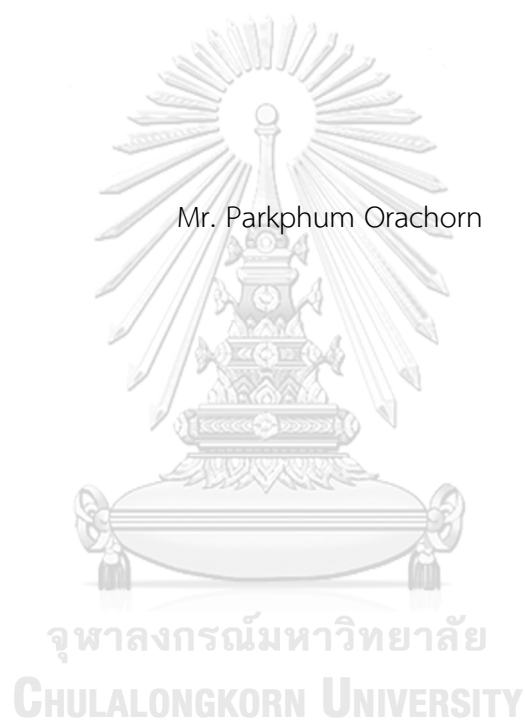
A Dissertation Submitted in Partial Fulfillment of the Requirements

for the Degree of Doctor of Engineering Program in Nuclear Engineering

Department of Nuclear Engineering

Faculty of Engineering

Chulalongkorn University

Academic Year 2017

Thesis Title	DEVELOPMENT OF TECHNIQUE FOR SCREENING LIQUIDS IN UNOPENED BOTTLE USING LOW ENERGY X-RAY TRANSMISSION
By	Mr. Parkphum Orachorn
Field of Study	Nuclear Engineering
Thesis Advisor	Associate Professor Nares Chankow
Thesis Co-Advisor	Associate Professor Somyot Srisatit

Accepted by the Faculty of Engineering, Chulalongkorn University in Partial Fulfillment of the Requirements for the Doctoral Degree

--Dean of the Faculty of Engineering

(Associate Professor Supot Teachavorasinskun, D.Eng.)

THESIS COMMITTEE

--Chairman

(Associate Professor Sunchai Nilsuwankosit, Ph.D.)

--Thesis Advisor

(Associate Professor Nares Chankow)

--Thesis Co-Advisor

(Associate Professor Somyot Srisatit)

--Examiner

(Associate Professor Supitcha Chanyotha, Ph.D.)

--Examiner

(Assistant Professor Somboon Rassame, Ph.D.)

--External Examiner

(Sarinrat Wonglee, D.Eng.)

ภาคภูมิ อรชร : การพัฒนาเทคนิคสำหรับการคัดกรองของเหลวในภาชนะปิดโดยใช้การทะลุผ่านของรังสีเอกซ์พลังงานต่ำ (DEVELOPMENT OF TECHNIQUE FOR SCREENING LIQUIDS IN UNOPENED BOTTLE USING LOW ENERGY X-RAY TRANSMISSION) อ.ที่ปรึกษาวิทยานิพนธ์หลัก: รศ. นเรศร์ จันทน์ขาว, อ.ที่ปรึกษาวิทยานิพนธ์ร่วม: รศ. สมยศ ศรีสถิตย์, หน้า.

เมื่อปี 2549 มีการเปิดเผยแผนการก่อการร้ายที่สนามบินอังกฤษโดยใช้วัตถุระเบิดเหลว จากนั้นมาสายการบินจึงมีการกำหนดมาตรการการนำของเหลวขึ้นเครื่องบินโดยของเหลวที่สามารถนำขึ้นเครื่องบินได้ต้องบรรจุอยู่ในภาชนะขนาดไม่เกิน 100 มิลลิลิตร และรวมกันได้ไม่เกิน 1,000 มิลลิลิตร งานวิจัยนี้ได้ทำการทดลองเพื่อใช้ในการตรวจสอบและป้องกันของเหลวที่เป็นอันตรายอาทิเช่น น้ำมันเชื้อเพลิง แอลกอฮอล์ ไฮโดรเจนเปอร์ออกไซด์ และของเหลวที่ติดไฟได้หรือเป็นสารตั้งต้นสำหรับทำวัตถุระเบิดเหลว โดยใช้เทคนิคการทะลุผ่านของรังสีเอ็กซ์พลังงานต่ำในช่วง 13.6-43.5 กิโลอิเล็กตรอนโวลต์ จากต้นกำเนิดรังสีพลูโตเนียม-238 และใช้การคำนวณค่าสัมประสิทธิ์การทะลุผ่านของของเหลวในการตรวจและคัดแยกชนิดของของเหลว จากผลการวิจัยพบว่า สามารถคัดแยกของเหลวประเภทน้ำ แอลกอฮอล์ และน้ำมัน ออกจากกันได้เป็นอย่างดี โดยทั้งนี้ขึ้นอยู่กับพลังงานของรังสีที่ใช้ และขนาดของเส้นผ่านศูนย์กลางของภาชนะ เนื่องจากภาชนะมีขนาดและชนิดต่างๆกัน จึงใช้พลังงานของรังสีเอ็กซ์หลายพลังงานในทางปฏิบัติ ซึ่งเทคนิคนี้สามารถนำไปประยุกต์ใช้ในการคัดแยกและตรวจสอบของเหลวในภาชนะปิดเพื่อใช้ในสนามบินได้

จุฬาลงกรณ์มหาวิทยาลัย
CHULALONGKORN UNIVERSITY

ภาควิชา	วิศวกรรมนิวเคลียร์	ลายมือชื่อนิสิต	
สาขาวิชา	วิศวกรรมนิวเคลียร์	ลายมือชื่อ อ.ที่ปรึกษาหลัก	
ปีการศึกษา	2560	ลายมือชื่อ อ.ที่ปรึกษาร่วม	

5471447321 : MAJOR NUCLEAR ENGINEERING

PARKPHUM ORACHORN: DEVELOPMENT OF TECHNIQUE FOR SCREENING LIQUIDS IN UNOPENED BOTTLE USING LOW ENERGY X-RAY TRANSMISSION. ADVISOR: ASSOC. PROF. NARES CHANKOW, CO-ADVISOR: ASSOC. PROF. SOMYOT SRISATIT, pp.

Since August 2006 after the discovery of terrorists' attempts to explode airplanes with liquid explosives in United Kingdom, each airline passenger is allowed to carry only a maximum of 100 ml liquid in each container and a total of not more than 1,000 ml in carry-on luggage. This measure was adopted to prevent bringing sufficient amount of fuel oil, alcohol, hydrogen peroxide or other flammable and explosive liquids into the aircraft. In this research, X-ray transmission technique was experimentally investigated using low energy X-rays between 13.6 – 43.5 keV emitted from ^{238}Pu radioisotopic source and linear attenuation coefficient of liquids were calculated. The results indicated that the technique could clearly distinguish water, alcohol and fuel oil while its sensitivity is dependent upon radiation energy and diameter of the bottle. Other kinds of liquid are also tested. For bottles or containers having various diameters, multi-energy X-rays may be more practical. This technique is possible to employ the technique for screening bottled liquids contained in unopened bottles at airports.

Department:	Nuclear Engineering	Student's Signature	....
Field of Study:	Nuclear Engineering	Advisor's Signature	....
Academic Year:	2017	Co-Advisor's Signature	....

ACKNOWLEDGEMENTS

จุฬาลงกรณ์มหาวิทยาลัย
CHULALONGKORN UNIVERSITY

CONTENTS

จุฬาลงกรณ์มหาวิทยาลัย
CHULALONGKORN UNIVERSITY

LIST OF TABLES

LIST OF FIGURES

CHAPTER I

INTRODUCTION

1.1.Introduction

In 2006, the terrorist attempts to blow up several aircraft during flight using liquid explosives at London-Heathrow Airport, the European Commission created the rules on aviation security to fix the problem and prevent malicious threats.[1]

These rules restrict passengers on carrying liquids, aerosols and gels (LAGs)[2] past screening points, the restrictions are as follows:

•	Liquids in individual containers with volumes of not more than 100 ml packed in one transparent 1 litre re-sealable plastic bag as show in figure 1.1.
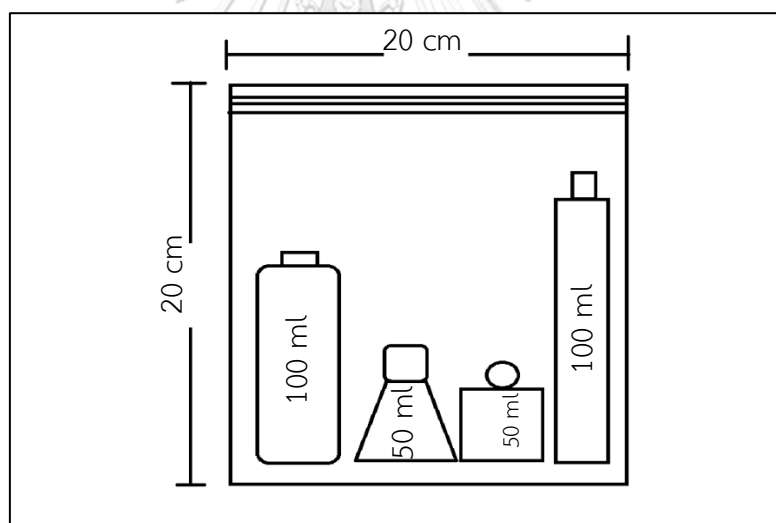
Figure 1.1 Liquids capacity and re-sealable plastic bag.

•	Liquids which are to be used during the trip for medical purposes or special dietary requirements, including baby food.

•	Duty free liquids must be packed in transparent plastic bag, which proof of purchase at airside at that airport on that day is displayed.

These rules may change in the future with the suitable technology for screening in liquid explosive.

For most convenience and safety, reliable methods and devices are needed to identify liquid in unopened bottles. Several methods have been introduced and tested such as vapor and trace detection, x-ray imaging[3], x-ray computed tomography (CT)[4], neutron techniques, nuclear magnetic resonance (NMR)[5], magnetic resonance imaging (MRI) and Raman spectroscopy[6] [7]. Each method has advantages and limitations.[8]

This research introduces a simple low energy x-ray and gamma-ray transmission technique to identify liquid types in unopened bottles. Low energy x-rays and gamma-rays in the range of approximately 10 to 120 keV emitted from radioisotope sources are experimentally investigated including ^{57}Co, ^{238}Pu and ^{241}Am. The transmitted intensity is measured with a compact and good resolution CdTe detector. The transmission factors of liquids contained in bottles of different sizes and thicknesses are investigated which are dependent upon liquid composition, diameter of bottle and photon energy.

1.2. Objective of Research

1.2.1 To develop a method to screen the liquids in an unopened bottle by using the low energy x-ray transmission.

1.3. Scope of the Research

1.3.1 Investigate the factors affecting the effectiveness of the x-ray transmission technique in screening the liquids such as the X-ray energy, the diameter, thickness and material of the bottle.

1.3.2 Liquids to be investigated are such as nitro-explosives, peroxides, flammables and water-based solutions.

1.3.3 Design prototype equipment to be used for screening of liquid in bottle at airports.

1.4. Research Methodology
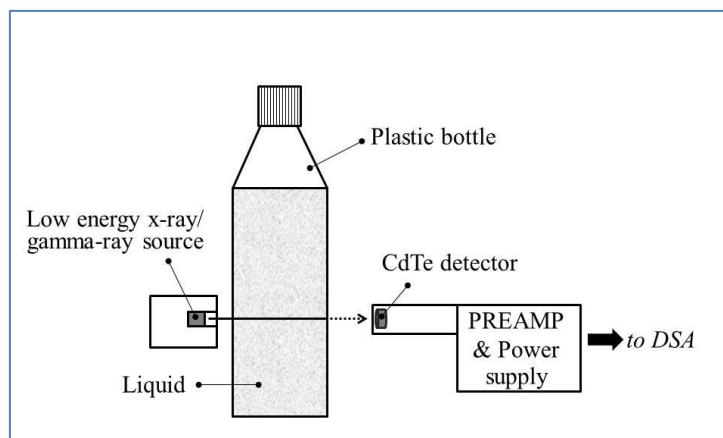
Figure 1.2 Experiment set-up.

Material

- Low energy x-ray / gamma-ray source
- CdTe detector
- PREAMP & Powersupply
- Collimator
- Bottles and Liquids
- Computer for analysis

Passengers may carry liquid in bottles with difference in sizes ranging from a few centimeters up to about 10 centimeters in diameter. In principle, lower energy should give better sensitivity but will have lesser penetrating power. To cover wide range of bottle size in screening at airport, multi-energy x-ray/gamma-ray is needed. Radioactive sources with activities in the range of 1-100 mCi (37 MBq – 3.7 GBq) are tested for this purpose including ^{57}Co, ^{109}Cd, ^{238}Pu and ^{241}Am. X- and gamma-rays are detected with a compact CdTe detector for good energy resolution but does not require cooling with liquid nitrogen. The source and the detector are positioned on the opposite side of the bottle under inspection to obtain transmitted x- and gamma-ray intensities.

Transmission factors for several kinds of liquids contained in bottles having diameters ranging from 2.26 to 8.75 cm are first investigated by using 13.6 - 20.1 keV U L x-rays from [238]Pu as well as 59.6 keV gammas from [241]Am source and 122 keV gammas from [57]Co. The ratio of transmitted intensities of ethyl alcohol, gasoline, and liquid explosive will compare with water (I_{XL}/I_{XW}). The attenuation coefficient will be calculated to identify liquid types.

1.5.Expected Benefits

The developed technique to screen the liquids in an unopened bottle by using the low energy x-ray transmission can be used for carry-on baggage inspection.

จุฬาลงกรณ์มหาวิทยาลัย

CHULALONGKORN UNIVERSITY

CHAPTER II

THEORY

2.1 Literature review

During the recent years, many techniques in explosive detection in the baggage were studied (K. Wells, D. Bradley: 2012)[9]. Such as x-ray scatter tomography by G. Harding (2004)[4] or x-ray transmission imaging(Q. Gonga, R.I. Stoianb, D. S. Coccarellia, J. A. Greenberga, E. Verac, M.E. Gehma: 2018)[3] but some explosive is liquids so it is hard to detect liquid explosive in an unopened bottle. Triacetone triperoxide (TATP) is one of the most dangerous liquid explosives because of it very sensitive to impact, flame or electric discharge (R. Matyas, J. Chylkova: 2013)[10]. C. Eliasson, N.A. Macleod, and P. Matousek (2007)[6] use Raman technique to inspect H_2O_2 30% that is liquid explosive mixture and Raman technique can inspect it. But H_2O_2 concentration for make TATP can be lower or higher(J.C. Oxley) [11].

The linear attenuation coefficient is a parameter that can identify material types by using Lambert's Law equation. S.M. Dongarge and S.R. Mitkar (2012)[12] determined a linear attenuation coefficient of alcohol and other solution but the value had a small difference because of they used x-ray energy 360 keV. S.M. Midgley (2004)[13] measured linear attenuation coefficient by using low x-ray energy in a range of 30-140 keV and the results give more different value from each material.

The aim of this work was to obtain the technique that can classify liquid explosive and other hazardous liquids including with flammable liquid and liquid explosive mixture by using low energy x-ray transmission.

2.2 Attenuation coefficient

The principle of the x-ray and gamma-ray transmission technique has been well understood i.e. the transmitted intensity (I_x) decreases exponentially with attenuation coefficient (μ) and thickness (x) of material according to Lambert's law. The attenuation coefficient decreases as x- or gamma-ray energy increases except at the absorption edge energy.
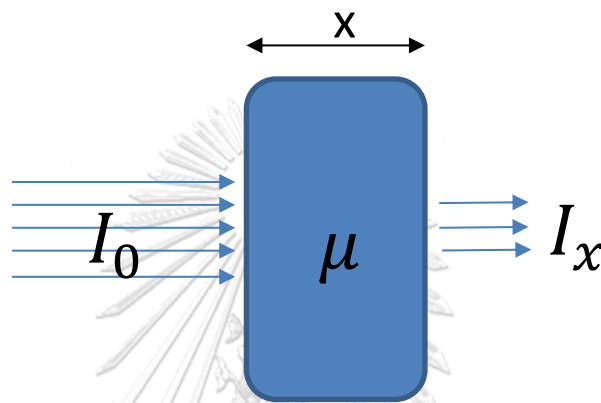
Figure 2.1 Parameters in Lambert's law calculation.

$$I = I_0 e^{-\mu x} \tag{2.1}$$

Where I_0 is intensity when there is no liquid in the bottle, I_x is transmitted intensity through liquid, x is thickness of liquid and μ is linear attenuation coefficient of liquid. For mixture, the attenuation coefficient can be simply calculated from equation2

$$\left(\frac{\mu}{\rho}\right)_{mix} = w_1 \left(\frac{\mu}{\rho}\right)_1 + w_2 \left(\frac{\mu}{\rho}\right)_2 + w_3 \left(\frac{\mu}{\rho}\right)_3 + \cdots \tag{2.2}$$

Where ρ is physical density, $\left(\frac{\mu}{\rho}\right)_{mix}$ is mass attenuation coefficient of mixture; $\left(\frac{\mu}{\rho}\right)_1$, $\left(\frac{\mu}{\rho}\right)_2$, $\left(\frac{\mu}{\rho}\right)_3$ are mass attenuation coefficients of components number 1, 2 and 3; and w1, w2, w3 are weight fractions of components number 1, 2, and 3 respectively[12, 14].

Theoretically, differences in the attenuation coefficients become larger at low energy, transmission of x- or gamma-ray may be applicable to inspect liquid types in

a bottle containing light elements such as water, alcohol, oil as well as other flammable and explosive liquids. [13]

2.3 Type of Hazardous Liquids[8]

Table 1.1 Some mono-component nitro-explosives and their main features.

Item	Chemical formula	Density(g/cm^3)	Vapor concentration (ppm)	Z_{eff}
Nitromethane	CH_3NO_2	1.137	36,630	7.033
Tetranitromethane	$C(NO_2)_4$	1.640	10,900	7.592
Nitroglycerine	$CHONO_2(CH_2NO_2)_2$	1.595	0.306	7.344
Ethylene glycol dinitrate	$(CH_2ONO_2)_2$	1.489	71.4	7.316
Diethy glycol dinitrate	$(CH_2CH_2ONO_2)_2O$	1.380	5.1	7.233

Table 1.2 Some multi-component nitro-explosives and their characteristics

Item	Chemical formula CocTaB	Z_{eff}
Helhofite	Nitrobenzol($C_6H_5NO_2$)(28%) and nitric acid (HNO_3) (72%)	7.32
Anergit	Dinitrobenzol ($C_6H_5(NO_2)_2$) (50%) and nitric acid (HNO_3)(50%)	7.22
Panclastit	Dinitrogen tetroxide (($NO_2)_2$)(65%)2carbon bisdulphide(CS_2)(35%)	
KD-mixture	Nitric acid (45%), dichloroethane(30%)2 oleum(25%)	

Table 1.3 Some explosive peroxide and peroxide nitro-explosives and their characteristics

Item	Chemical formula	Density (g/cm^3)	Z_{eff}
Triacetone triperoxide(TATP)	$C_9H_{18}O_6$	1.0-1.2	6.549
Hexamethylene triperoxide diamine (HMTD)	$C_6H_{12}O_6N_2$	0.6-0.9	6.769
Methyl ethyl ketone peroxide (MEKP)	$C_8H_{18}O_6$	1.0	6.486

Table 1.4 Different types of flammable liquid (carbon hydrates) and their characteristics

Item	Chemical formula	Density(g/cm^3)	Vapor concentration (ppm)	Z_{eff}
Gasoline	C_7H_{17}	0.76		5.375
Alcohol	C_2H_5OH	0.78	130,000 ppm (40 $^\circ$C)	6.043
Acetone	C_3H_6O	0.79	234,000 ppm (35 $^\circ$C)	6.034
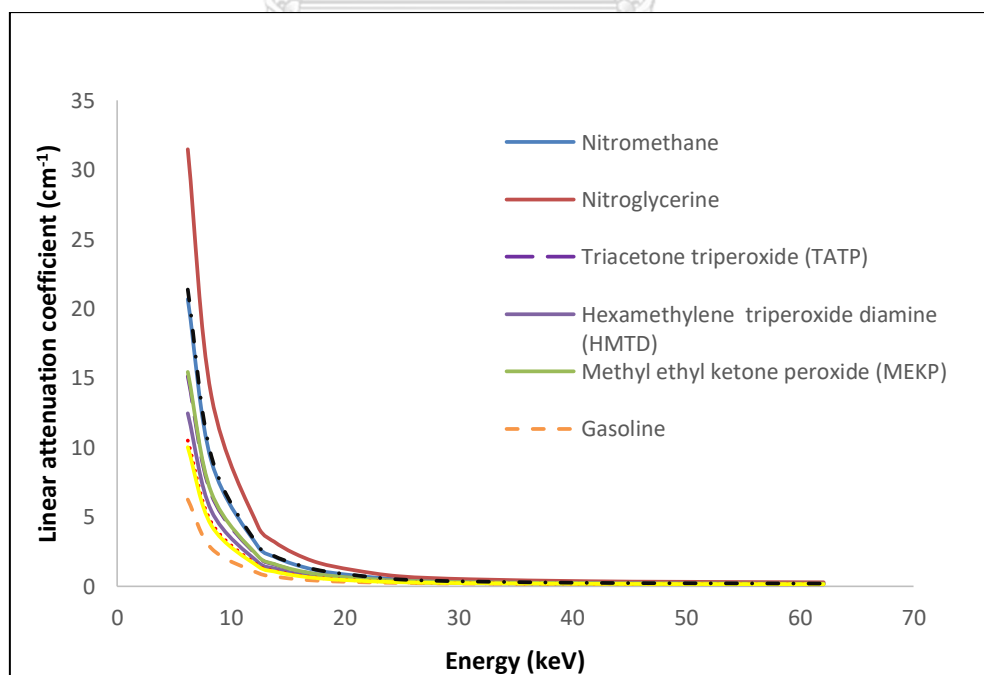
Figure 2. 2 Linear attenuation of hazardous liquids.

2.4 The Fundamental Law of Gamma-Ray Attenuation[15]

Figure 2.3 demonstrates a simple attenuation experiment. When gamma radiation of intensity I_0 is incident on an absorber of thickness L, the transmitted intensity (I) transmitted by the absorber is given by the equation.

$$I = I_0 e^{-\mu_l L} \tag{2.3}$$
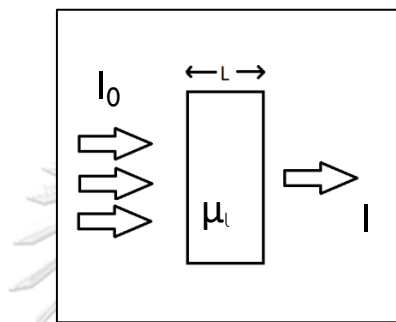
Figure 2.3 The fundamental law of gamma-ray attenuation. [15]

Where μ_l is the linear attenuation coefficient (expressed in cm^{-1}). The gamma-ray transmission can obtain from the ratio of I/I_0 . Figure 2.4 shows exponential attenuation for three different gamma-ray energies and the transmission increases with increasing gamma-ray energy and decreases with increasing absorber thickness. Measurements with different sources and absorbers show that the attenuation coefficient μ_l depends on the gamma-ray energy and the atomic number (Z) and density (ρ) of the absorber. For example, lead has a high density and atomic number and transmits a much lower fraction of incident gamma radiation than does a similar thickness of aluminum or steel. The attenuation coefficient in Equation 2.3 is called the linear attenuation coefficient. Figure 2.5 shows the linear attenuation of solid sodium iodide, a common material used in gamma-ray detectors.
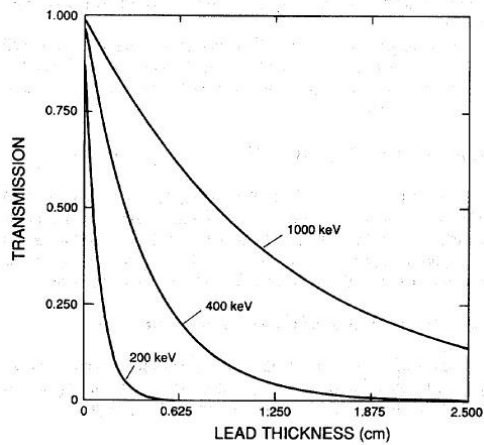
Figure 2.4 Transmission of gamma rays through lead absorbers.[15]

Alpha and beta particles have a well-defined range or stopping distance; however, as Figure 2.4 shows, gamma rays do not have a unique range. The reciprocal of the attenuation coefficient $1/\mu_l$ has units of length and is often called the mean free path. The mean free path is the average distance a gamma ray travels in the absorber before interacting.
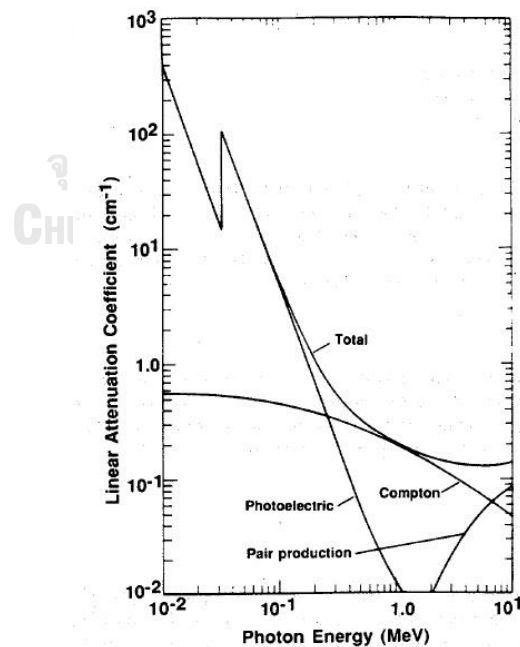
Figure 2.5 Linear attenuation coefficient of NaI showing contributions from photoelectric absorption, Compton scattering and pair production. [15]

2.4.1 Mass attenuation coefficient

The linear attenuation coefficient is the simplest absorption coefficient to measure experimentally, but it is not usually tabulated because of its dependence on the density of the absorbing material. For example, at a given energy, the linear attenuation coefficients of water, ice, and steam are all different, even though the same material is involved.

Gamma rays interact primarily with atomic electrons; therefore, the attenuation coefficient must be proportional to the electron density ρ, which is proportional to the bulk density of the absorbing material. However, for a given material the ratio of the electron density to the bulk density is a constant, Z/A, independent of bulk density. The ratio Z/A is nearly constant for all except the heaviest elements and hydrogen.

$$P = \frac{Z\rho}{A}$$
2.4)

where P = electron density

Z = atomic number

ρ = mass density

A = atomic mass

The ratio of the linear attenuation coefficient to the density (μ_l/ρ) is called the mass attenuation coefficient μ and has the dimensions of area per unit mass (cm^2/g). The units of this coefficient hint that one may think of it as the effective cross-sectional area of electrons per unit mass of absorber. The mass attenuation coefficient can be written in terms of a reaction cross section, σ (cm^2):

$$\mu = \frac{N_0\sigma}{A}$$
2.5)

Where No is Avogadro's number (6.02×10^{23}) and A is the atomic weight of the absorber. The cross section is the probability of a gamma ray interacting with a single atom. Using the mass attenuation coefficient, Equation 2.3 can be rewritten as;

$$I = I_0 e^{-\mu \rho L} = I_0 e^{-\mu x} \qquad 2.6)$$

Where x = ρL

The mass attenuation coefficient is independent of density for the example mentioned above; water, ice, and steam all have the same value of p. This coefficient is more commonly tabulated than the linear attenuation coefficient because it quantifies the gamma-ray interaction probability of an individual element. The mass attenuation coefficient for compound materials can be calculated by the equation.

$$\mu = \sum \mu_i W_i \qquad 2.7)$$

Where μ_i = mass attenuation of the ith element.

W$_i$ = weight fraction of th i[th] element.

Interaction process

The gamma rays of interest to NDA applications fall in the range 10 to 2000 keV and interact with detectors and absorbers by three major processes: photoelectric absorption, Compton scattering, and pair production. In the photoelectric absorption process, the gamma ray loses all of its energy in one interaction. The probability for this process depends very strongly on gamma-ray energy E_γ and atomic number Z. In Compton scattering, the gamma ray loses only part of its energy in one interaction. The probability for this process is weakly dependent on E and Z. The gamma ray can lose all of its energy in one pair-production interaction. However, this process is relatively unimportant for fissile material assay since it has a threshold above 1 MeV.

2.4.2 Photoelectric absorption

A gamma ray may interact with a bound atomic, electron in such a way that it loses all of its energy and ceases to exist as a gamma ray. Some of the gamma-ray energy is used to overcome the electron binding energy, and most of the remainder is transferred to the freed electron as kinetic energy. A very small amount of recoil energy remains with the atom to conserve momentum. This is called photoelectric absorption because it is the gamma-ray analog of the process discovered by Hertz in 1887 whereby photons of visible light liberate electrons from a metal surface. Photoelectric absorption is important for gamma-ray detection because the gamma ray gives up all its energy, and the resulting pulse falls in the full-energy peak.
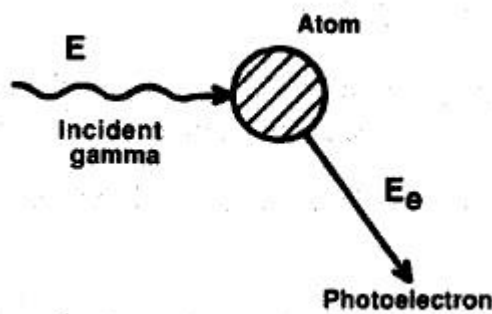
Figure 2.6 A schenratic representation of the photoelectric absorption process. [15]

The probability of photoelectric absorption depends on the gamma-ray energy, the electron binding energy, and the atomic number of the atom. The probability is greater the more tightly bound the electron therefore, K electrons are most affected (over 80% of the interactions involve K electrons), provided the gamma-ray energy exceeds the K-electron binding energy. The probability is given approximately by Equation 2.8, which shows that the interaction is more important for heavy atoms like lead and uranium and low-energy gamma rays:

$$\tau \propto Z^4/E^3 \qquad\qquad 2.8)$$

Where τ = photoelectric, mass attenuation coefficient.

This proportionality is only approximate because the exponent of Z varies in the range 4.0 to 4.8. As the gamma-ray energy decreases, the probability of photoelectric absorption increases rapidly (see Figure 7). Photoelectric absorption is the predominant interaction for low-energy gamma rays, X-rays, and bremsstrahlung. The energy of the photoelectron E. released by the interaction is the difference between the gamma-ray energy E_γ and the electron binding energy E_b:

$$E_e = E_\gamma - E_b \qquad\qquad 2.9)$$

In most detectors, the photoelectron is stopped quickly in the active volume of the detector, which emits a small output pulse whose amplitude is proportional to the energy deposited by the photoelectron. The electron binding energy is not lost but appeiys as characteristic X-rays emitted in coincidence with the photoelectron. In most cases, these X-rays are absorbed in the detector in coincidence with the photoelectron and the resulting output pulse is proportional to the total energy of the incident gamma ray. For low-energy gamma rays in very small detectors, a sufficient number of K X-rays can escape from the detector to cause escape peaks in the observed spectrum; the peaks appear below the full-energy peak by an amount equal to the energy of the X-ray.

Figure 2.7 shows the photoelectric mass attenuation coefficient of lead. The interaction probability increases rapidly as energy decreases, but then becomes much smaller at gamma-ray energy just below the binding energy of the K electron. This discontinuity is called the K edge below this energy the gamma ray does not have sufficient energy to dislodge a K electron. Below the K edge the interaction probability increases again until the energy drops below the binding energies of the L electron; these discontinuities are called the LI, LII, and LIII edges. The presence of these absorption edges is important for densitometry and x-ray fluorescence measurements.
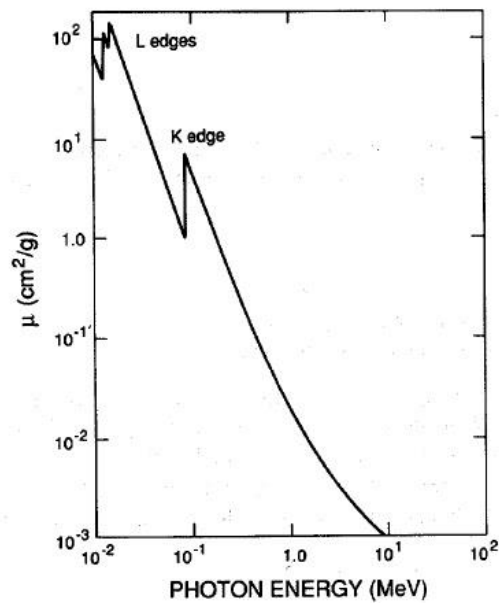
Figure 2.7 Photoelectric mass attenuation coefficient of lead. [15]

2.4.3 Compton scattering

Compton scattering is the process whereby a gamma ray interacts with a free or weakly bound electron ($E_\gamma \gg E_b$) and transfers part of its energy to the electron (see Figure 2.8).

Conservation of energy and momentum allows only a partial energy transfer when the electron is not bound tightly enough for the atom to absorb recoil energy. This interaction involves the outer, least tightly bound electrons in the scattering atom. The electron becomes a free electron with kinetic energy equal to the difference of the energy lost by the gamma ray and the electron binding energy. Because the electron.
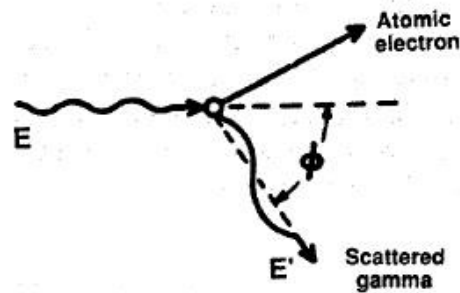
Figure 2.8 A schematic representation of Compton scattering. [15]

Binding energy is very small compared to the gamma-ray energy, the kinetic energy of the electron is very nearly equal to the energy lost by the gamma ray:

$$E_e = E_\gamma - E' \qquad \qquad 2.10)$$

Where E_e = energy of scattered electron

E_γ = energy of incident gamma ray

E' = energy of scattered gamma ray.

Two particles leave the interaction site: the freed electron and the scattered gamma ray. The directions of the electron and the scattered gamma ray depend on the amount of energy transferred to the electron during the interaction. Equation 2.11 gives the energy of the scattered gamma ray; Figure 2.9 shows the energy of the scattered electron as a function of scattering angle and incident gamma-ray energy.

$$E' = m_0 c^2 / (1 - cos\emptyset + \frac{m_0 c^2}{E}) \qquad \qquad 2.11)$$

where $m_o c^2$ = rest energy of electron = 511 keV

φ = angle between incident and scattered gamma rays (see Figure 2.9)

This energy is minimum for a head-on collision where the gamma ray is scattered 180°and the electron moves forward in the direction of the incident gamma ray. For this case the energy of the scattered gamma ray is given by Equation 2.12 and the energy of the scattered electron is given by Equation 2.13:

$$E'(min) = \frac{m_0 c^2}{\left(2 + \frac{m_0 c^2}{E}\right)} \qquad \qquad 2.12)$$

$$\cong \frac{m_0 c^2}{2} = 256 \; keV; if \; E \gg m_0 c^2/2$$

$$E_e(max) = \frac{E}{\left[1 + \frac{m_0 c^2}{(2E)}\right]} \qquad 2.13)$$

$$\cong E - \frac{m_0 c^2}{2} = E - 256\ keV; if\ E \gg m_0 c^2/2$$
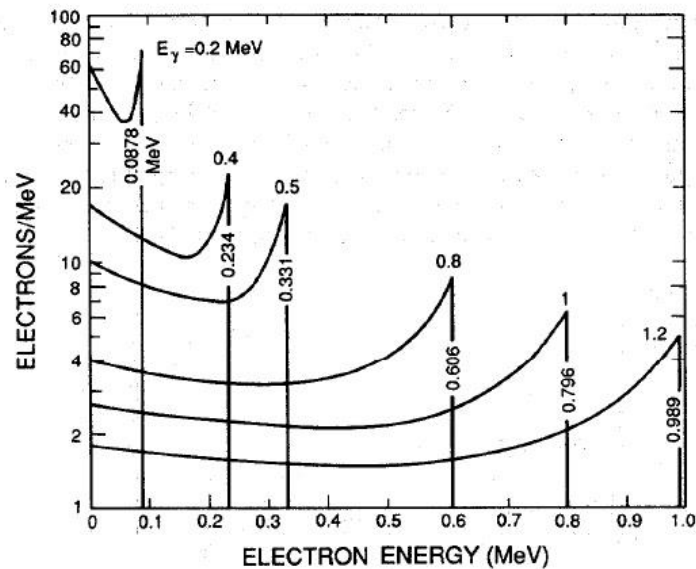
Figure 2.9 Energy of Compton-scattered electrons as a function of scattering angle and incident gamma-ray energy (E_γ). The sharp discontinuity corresponds to the maximum energy that can be transferred in a single scattering. [15]

For very small angle scatterings ($\phi \approx 0°$), the energy of the, scattered gamma ray is only slightly less than the energy of the incident gamma ray and the scattered electron takes very little energy away from the interaction. The energy given to the scattered electron ranges from near zero to the maximum given by Equation 2.13. When a Compton scattering occurs in a detector, the scattered electron is usually stopped in the detection medium and the detector produces an output pulse that is proportional to the energy lost by the incident gamma ray. Compton scattering in a detector produces a spectrum of output pulses from zero up to the maximum energy given by Equation 2.13. It is difficult to relate the Compton-scattering spectrum to the energy of the incident gamma ray. Figure 2.10 shows the measured gamma-ray spectrum from a monoenergetic gamma-ray source (^{137}Cs). The full-

energy peak at 662 keV is formed by interactions where the gamma ray loses all of its energy in the detector either by a single photoelectric absorption or by a series of Compton scattering followed by photoelectric absorption. The spectrum of events below the full-energy peak is formed by Compton scattering where the gamma ray loses only part of its energy in the detector. The step near 470 keV corresponds to the maximum energy that can be transferred to an electron by a 662-keV gamma ray in a single Compton scattering. This step is called a Compton edge the energy of the Compton edge is given by Equation 2.13 and plotted in Figure 2.11. The small peak at 188 keV in Figure 12 is called a backscatter peak. The backscatter peak is formed when the gamma ray undergoes a large-angle scattering ($\approx$ 180°) in the material surrounding the detector and then is absorbed in the detector. The energy of the backscatter peak is given by Equation 2.12, which shows that the maximum energy is 256 keV. The sum of the energy of the backscatter peak and the Compton edge equals the energy of the incident gamma ray. Both features are the result of large-angle Compton scattering of the incident gamma ray. The event contributes to the backscatter peak when only the scattered gamma ray deposits its energy in the detection it contributes to the Compton edge when only the scattered electron deposits its energy in the detector.
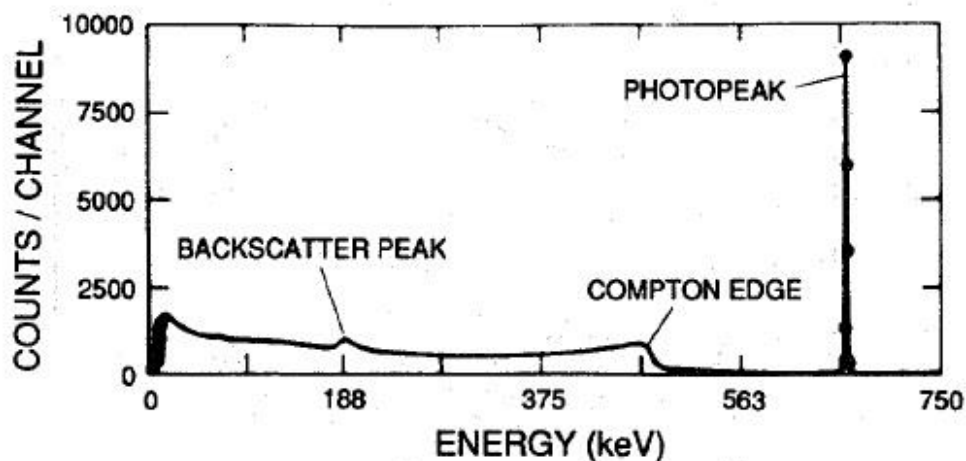
Figure 2.10 High-resolution spectrum of ^{137}Cs showing full-energy photopeak, Compton edge, and backscatter peak from the 662-keV gamma ray. Events below the photopeak are caused by Compton scattering in the detector and surrounding materials.[15]

Because Compton scattering involves the least tightly bound electrons, the nucleus has only a minor influence and the probability for interaction is nearly independent of atomic number. The interaction probability depends on the electron density, which is proportional to Z/A and nearly constant for all materials. The Compton-scattering probability is a slowly varying function of gamma-ray energy (see Figure 2.5).

2.4.4 Pair production

A gamma ray with energy of at least 1.022 MeV can create an electron-positron pair when it is under the influence of the strong electromagnetic field in the vicinity of a nucleus (see Figure 13). In this interaction the nucleus receives a very small amount of recoil energy to conserve momentum, but the nucleus is otherwise unchanged and the gamma ray disappears. This interaction has a threshold of 1.022 MeV because that is the minimum energy required to create the electron and positron. If the gamma ray energy exceeds 1.022 MeV, the excess energy is shared between the electron and positron as kinetic energy. This interaction process is relatively unimportant for nuclear material assay because most important gamma-ray signatures are below 1.022 MeV.
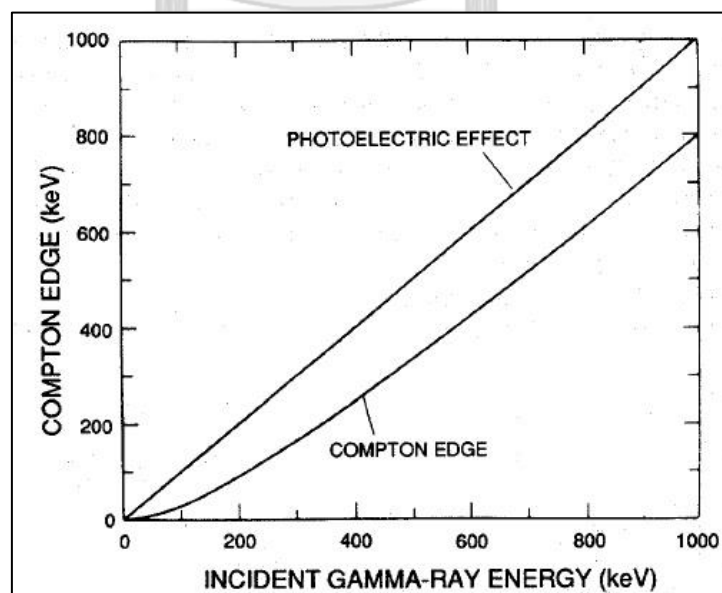
Figure 2.11 Energy of the Compton edge versus the energy of the incident gamma-ray.[15]
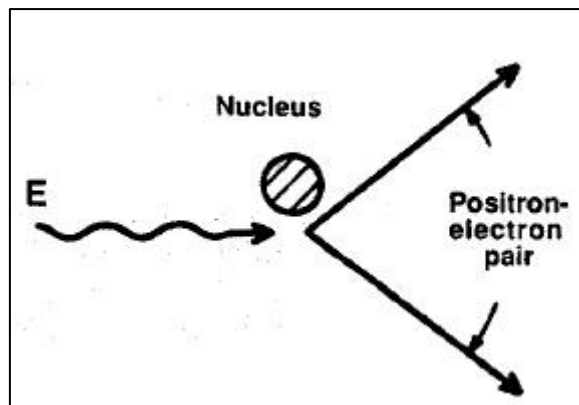
Figure 2.12 A schematic representation of pair production.[15]

The electron and positron from pair production are rapidly slowed down in the absorber. After losing its kinetic energy, the positron combines with an electron in an annihilation process, which releases two gamma rays with energies of 0.511 MeV. The lower energy gamma rays may interact further with the absorbing material or may escape. In a gamma-ray detector, this interaction often gives three peaks for a high-energy gamma ray (see Figure 2.13). The kinetic energy of the electron and positron is absorbed in the detector. One or both of the annihilation gamma rays may escape from the detector or they may both be absorbed. If both annihilation gamma rays are absorbed in the detector, the interaction contributes to the full-energy peak in the measured spectrum; if one of the annihilation gamma rays escapes from the detector, the interaction contributes to the single-escape peak located 0.511 MeV below the full-energy peak; if both gamma rays escape, the interaction contributes to the double-escape peak located 1.022 MeV below the full-energy peak. The relative heights of the three peaks depend on the energy of the incident gamma ray and the size of the detector. 'These escape peaks may arise when samples of irradiated fuel, thorium, and ^{232}U are measured because these materials have important gamma rays above the pair-production threshold. Irradiated fuel is sometimes measured using the 2186-keV gamma ray from the fission-product ^{144}Pr. The gamma-ray spectrum of ^{144}Pr in Figure 2.13 shows the single- and double-escape peaks that arise from pair-production interactions of the 2186-keV gamma ray in a germanium detector.
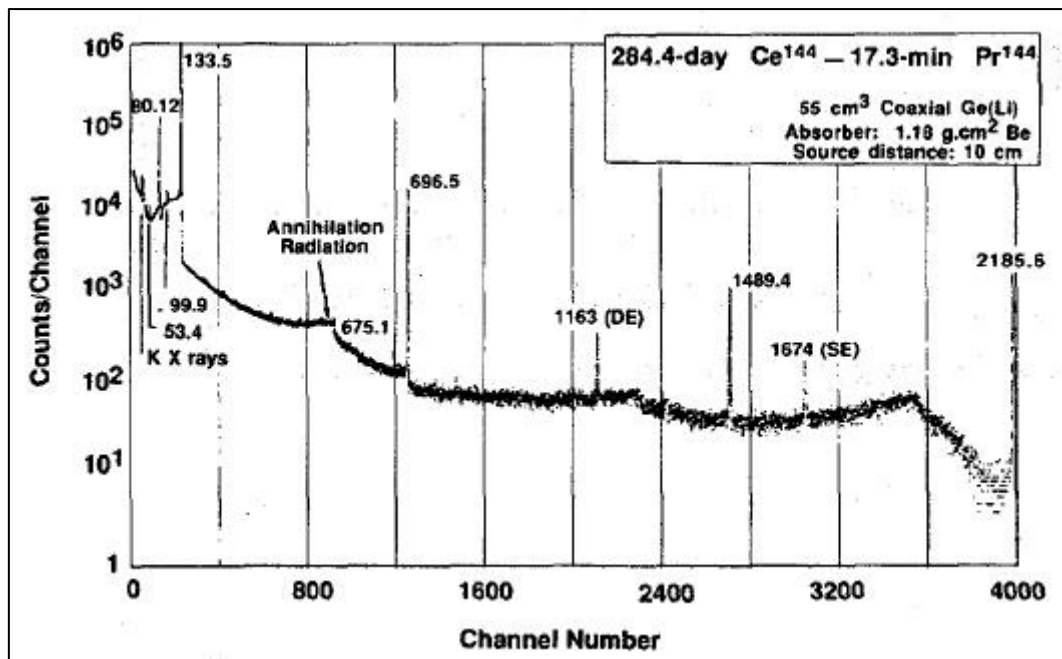
Figure 2.13 Gamma-ray spectrum of the fission-product [144]Pr showing single-escape (SE) and double-escape (DE) peaks (1674 and 1163) that arise from pair-production interactions of 2186-keV gamma rays in a germanium detector.[15]

Pair production is impossible for gamma rays with energy less than 1.022 MeV. Above this threshold, the probability of the interaction increases rapidly with energy (see Figure 7). The probability of pair production varies approximately as the square of the atomic number Z and is significant in high-Z elements such as lead or uranium. In lead, approximately 20% of the interactions of 1.5-MeV gamma rays are through the pair-production process, and the fraction increases to 50% at 2.0 MeV. For carbon, the corresponding interaction fractions are 2% and 4%.

2.5 Ultrasonic testing

Ultrasonic Testing (UT) uses high frequency sound waves (between 0.5 and 15 MHz) to conduct examinations and make measurements. Besides its wide use in engineering application (such as flaw detection/evaluation, dimensional measurements, material characterization, etc.), ultrasonic are also used in the medical field (such as sonography, therapeutic ultrasound, etc.).

In general, ultrasonic testing is based on the capture and quantification of either the reflected waves (pulse-echo) or the transmitted waves (through-

transmission). Each of the two types is used in certain applications, but generally, pulse echo systems are more useful since they require one-sided access to the object being inspected. [16]

2.5.1 Basic principles

A typical pulse-echo UT inspection system consists of several functional units, such as the pulser/receiver, transducer and a display device. A pulser/receiver is an electronic device that can produce high voltage electrical pulses. Driven by the pulser, the transducer generates high frequency ultrasonic energy. The sound energy is introduced and propagates through the materials in form of waves. When there is a discontinuity (such as a crach) in the wave path, part of the energy will be reflected back from the flaw surface. The reflected wave signal is transformed into an electrical signal by the transducer and is displayed on a screen. Knowing the velocity of the waves, travel time can be directly related to the distance that the signal traveled. From the signal, information about the reflector location, size, orientation and other features can sometimes be gained.

2.5.2 Advantage and disadvantages [16]

The primary advantages and disadvantages when compared to other NDT methods are:

Advantages

- It is sensitive to both surface and subsurface discontinuities.
- The depth of penetration for flaw detection or measurement is superior to other NDT methods.
- Only single-side access is needed when the pulse-echo technique is used.
- It is highly accurate in determining the reflector position and estimating its size and shape.
- Minimal part preparation is required.
- It provides instantaneous results.
- Detailed images can be produced with automated systems.

- It is nonhazardous to operators or nearby personnel and does not affect the material being tested.

- It has other used, such as thickness measurement, in addition to flaw detection.

- Its equipment can be highly portable or highly automated.

Disadvantages[16]

- Surface must be accessible to transmit ultrasound.

- Skill and training is more extensive than with some other methods.

- It normally requires a coupling medium to promote the transfer of sound energy into the test specimen.

- Materials that are rough, irregular in shape, very small, exceptionally thin or not homogenous are difficult to inspect.

- Cast iron and other coarse grained materials are difficult to inspect due to low sound transmission and high signal noise.

- Linear defects oriented parallel to the sound beam may go undetected.

- Reference standards are required for both equipment calibration and the characterization of flaws.

2.6 X-ray sources and x-ray detectors

- X-ray sources [17] [18] [19]

X-ray sources can be divided into 2 groups i.e. x-ray tubes and isotopic x-ray sources. The x-ray tubes produce x-rays from acceleration of electron in vacuum tube. Continuous x-rays are emitted from interaction of fast electrons with the anode target which are so called "bremsstrahlung" in German or "braking radiation" in English. This research intends to use an isotopic x-ray source due to its compact size and constant output. Moreover, it does not require electricity to generate x-rays. The isotopic x-ray sources are mostly radioactive isotopes produced by nuclear reactors and particle accelerators. There are various choices to be selected for

specific applications depending mainly upon the required energy range. Common x-ray isotopic sources are tabulated in Table 2.1

Table 2.1 Common low energy x-ray and gamma-ray sources

Isotope	Half-life	Major x-ray energy emitted and relative intensity
^{55}Fe	2.7 years	Mn K x-rays 5.90-6.49 keV (26%)
^{57}Co	0.74 year	Fe K x-rays 6.4-7 keV (55%) 14.41 keV gammas (9.5%) 122 keV gammas (85.6%) 136 keV gamma (10.6%)
^{109}Cd	1.24 years	Ag K x-rays 22.1 – 25.0 keV (100%) 88 keV gammas (3.6%)
^{238}Pu	87.7 years	U L x-rays 13.6-20.1 keV (13%) 43.5 keV gammas (0.39%)
^{241}Am	243 years	Np L x-rays 14-21 keV (40%)

Note: The energy below 10 keV is available only when Be is used as the source window

This research prefers an x-ray source that gives low energy x-rays and/or gamma-rays in 10 – 50 keV range so that photons can penetrate through liquid contained in bottle and still give difference in transmitted intensity for different kinds of liquid. From the data in Table 2.1, ^{109}Cd, ^{238}Pu and ^{241}Am are appropriate.

- X-ray detectors[18] [20]

At present, various types of detectors are available for detection of x-rays and gamma-rays. They are categorized into 3 groups including gas proportional, scintillation and semiconductor detectors as summarized in Table 2.2. Their detection efficiencies are illustrated in figure 2.14 – 2.15. It must be kept in mind that the efficiency at low energy is dependent upon thickness of the detector window while at high energy is dependent upon thickness and diameter of detector material.

Table 2.2 Detectors for x-rays and gamma-rays

Type of detector	Characteristics	Example
Proportional counter	good resolution, suitable for energy up to about 30 keV	Ar-filled, Kr-filled, Xe-filled detectors
Scintillation detector	poor energy resolution, available for energy from about 10 keV up to several MeV depending mainly on thickness of the crystal	- NaI(Tl) for 10 keV-10 MeV - Bismuth germinate(BGO) for 100 keV up to 10 MeV, poorer energy resolution, higher efficiency for high energy range
Semiconductor	excellent resolution, available for energy from a few keV up to several MeV depending on detector thickness and material	- Si(Li) for <1 keV up to 30 keV* - HPGe for 1 keV up to 10 MeV* - CdTe for 1 keV up to 100 keV** - CdZnTe for 10 keV up to 1 MeV** - Si PIN photodiode for 1 keV up to 30 keV**

Note: * needs liquid nitrogen, electrical or mechanical cooling
       ** compact size, only Peltier cooling is sufficient
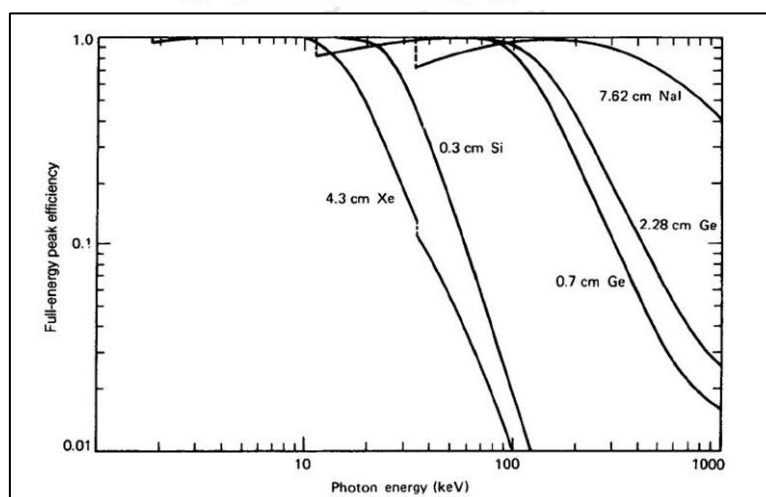
(a)
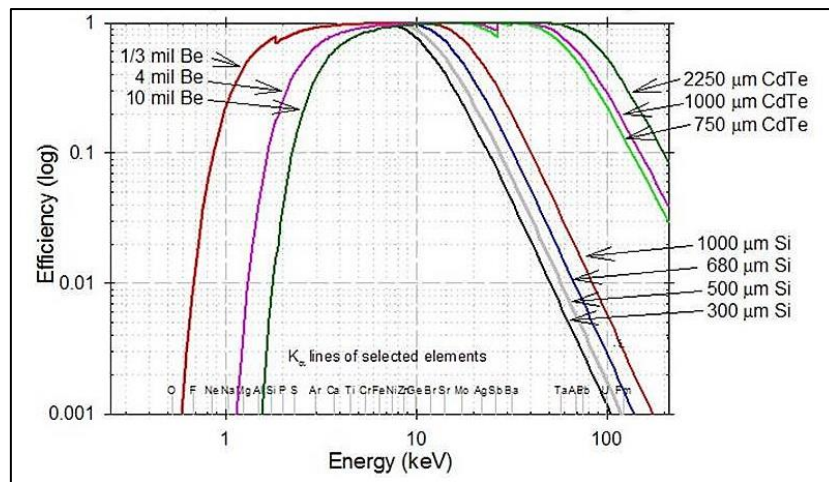
(b)

Figure 2.14 Comparison of intrinsic efficiencies of x-ray detectors (a) Xe-filled
proportional, Si(Li), HPGe and NaI(Tl) (b) Si PIN diode and CdTe [20]
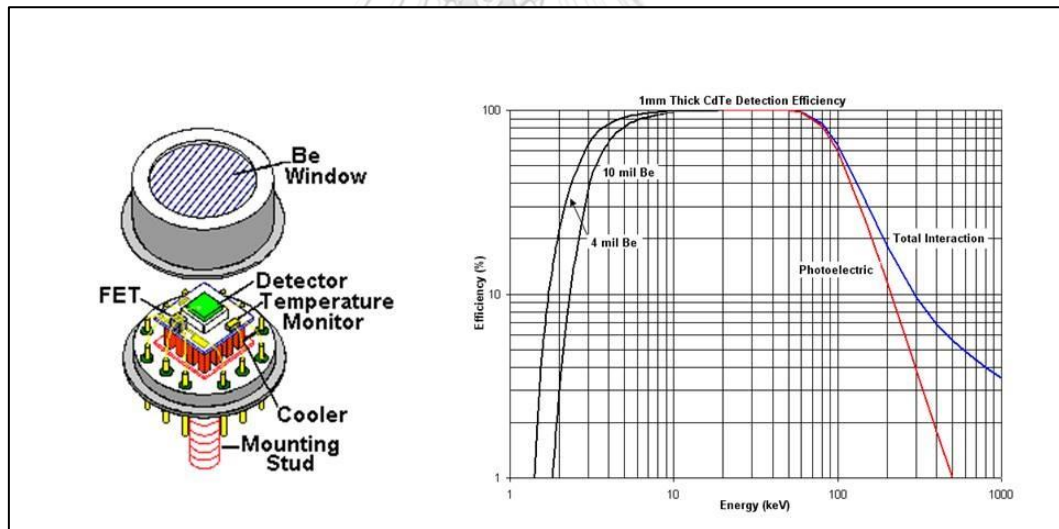
Figure 2.15 CdTe detector structure (left) and its intrinsic efficiency curve (right) [21]

CHAPTER III

EXPERIMENT

Factors that affected in the linear attenuation coefficient calculation were studied including x-ray energy, bottle diameter, bottle thickness and bottle types. The Lambert's Law was used for calculation of the linear attenuation coefficient of liquid that can be used to identify or classify types of liquid.

Equipment and materials:
- ^{238}Pu (13.6, 17.2, 20.1 and 43.5 keV) radioisotopic point source
- ^{241}Am (59.5 keV) radioisotope point source
- ^{57}Co (122 keV) radioisotope point source
- Copper collimators of aperture 5 mm ϕ
- CdTe-diode detector (detector areas 5 mm x 5 mm) model XR-100T with preamplifier
- Power supply
- ORTEC EASY-MCA 2k Multichannel Analyzer
- INSPEX Ultrasonic thickness gauge model IPX -251S
- Vernier caliper
- PET and HDPE plastic bottles
- Glass bottles
- Metal cans (aluminum and steel)
- Beverages and hazardous liquids
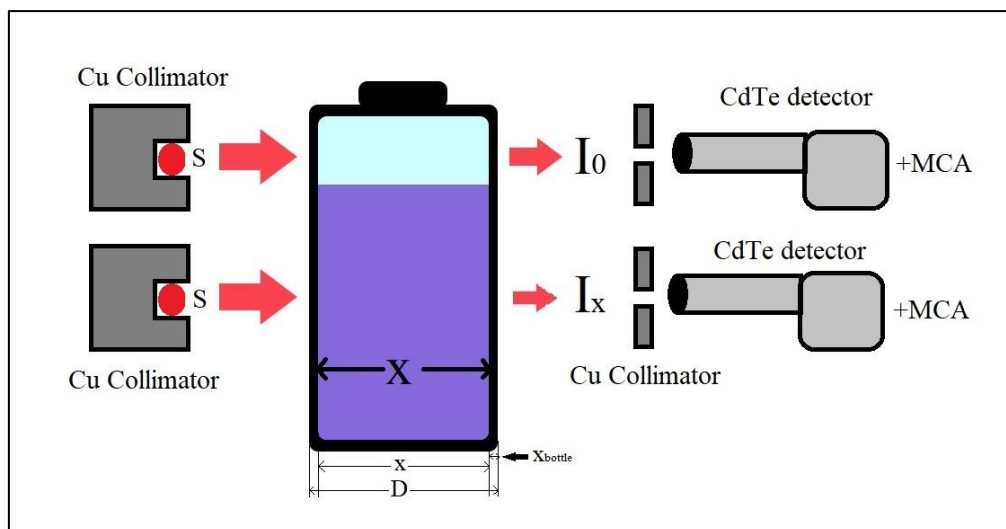
Figure 3.1 Experimental setup for determining the linear attenuation coefficients of liquids

The diagram of experimental setup for measuring the linear attenuation coefficient of liquids by using low energy x-ray transmission technique is shown in Figure 3.1. Three point sources including 100 mCi ^{241}Am (59.54 keV), 10 mCi ^{238}Pu (13.6, 17.2, 20.1 and 43.5 keV) and 10 mCi ^{57}Co (122 keV) were used to generate primary x-rays and gamma-rays in the range of about 13 to 122 keV. Copper collimators having aperture of 5 mm were selected for the source and the detector, instead of Pb, to avoid interference from Pb x-rays. A 5 mm x5 mm CdTe-diode detector model XR-100T-CeTe coupled with an ORTEC EASY-MCA 2k multichannel analyzer was employed for collecting x-ray and gamma- ray intensity. The source and the detector are positioned on the opposite side of the bottle under inspection to obtain transmitted x-ray and gamma-ray intensities.

3.1 Effect of x-ray energy

Theoretically, the linear attenuation coefficients of elements have large difference at low energy and get closer at high energy. Thus, in the first experiment, we experimented with three available radioisotope sources to observe their sensitivities and penetrating power.

The sources including ^{238}Pu (13.6 keV, 17.2 keV, 20.1 keV), ^{241}Am (59.5 keV) and ^{57}Co (122 keV) were used. The bottle was placed between the source and the

detector as in figure 3.1 then I_0 was measured near the top of the bottle where there was no liquid. The transmitted intensity (I_x) was measured at any position where there was liquid in the bottle. The counting time was 300 seconds. The tested samples were drinking water, soft drink, ethanol70%, kerosene, diesel and bensene95 contained in the same type of PET plastic bottle with outside diameter of 3.1 cm and bottle thickness of 0.06 cm (measured by Vernier caliper). The collimator was designed in the way that all the three sources could be put together allowing single measurement for all energy ranges. The experimental setup is shown in Figure 3.3

Figure 3.2 Copper collimator of aperture 2, 3 and 5 mm.
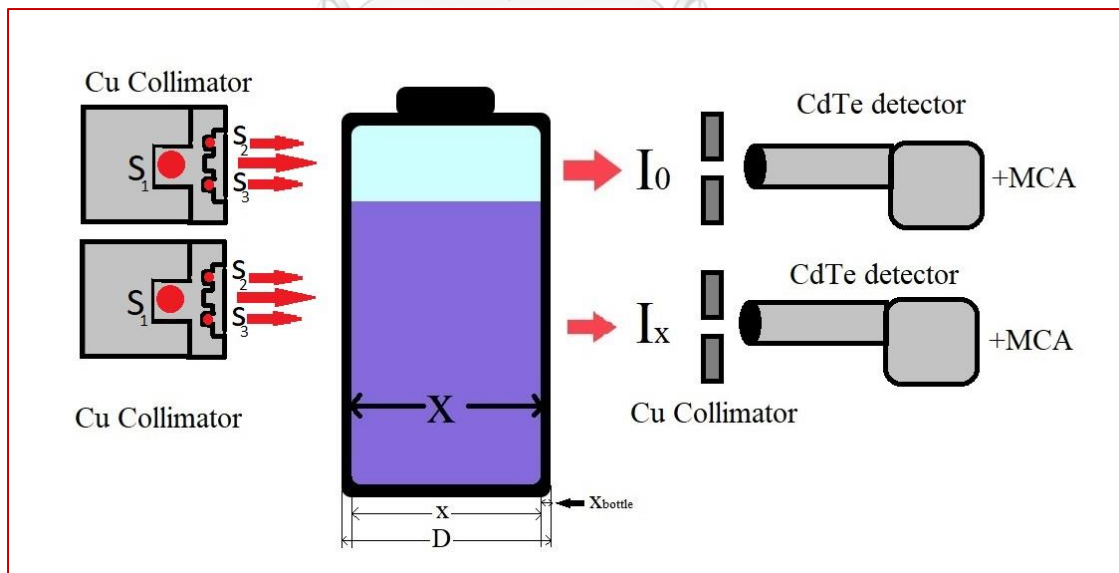
Figure 3.3 Experimental setup for investigating the effect of x-ray energy on the obtained linear attenuation coefficients of liquid

(S_1 is ^{238}Pu, S_2 is ^{241}Am and S_3 is ^{57}Co)

3.2 Effect of bottle diameter

Because there are many kinds of liquid bottles such as plastic and glass bottles with different diameters ranging from approximately 2 to 10 cm. To investigate the effect of bottle diameter, PET bottles with diameters of 2.26, 3.10, 3.33, 3.82, 4.96 and 7.40 cm were first selected. The bottles containing drinking water, soft drink, beer, ethanol (70%), kerosene, diesel, benzene 95, gasohol 95, gasohol E20 and gasohol E85 were placed between the source and the detector as in figure 3.1 for measurements of I_0 and I_x one after the other. Diameter and thickness of the PET bottles were measured by a Vernier caliper in order to find the exact liquid thickness (x). Only the ^{238}Pu source was used in this experiment because it gave satisfactory sensitivity in the previous experiment in comparison to the other two sources. The ^{57}Co gamma-ray energies (122 and 136 keV) were too high for those ranges of liquid thickness resulting in decreasing of the sensitivity. The available ^{241}Am source used in the previous experiment had too thick window allowing only 59.5 keV gammas to come out which was also too high for those range of liquid thickness. The energies of Np L x-rays from ^{241}Am were actually very close to those from the ^{238}Pu but the source window had to be made of thin beryllium (Be) to allow them to come out. Thus, the ^{57}Co and ^{241}Am sources were not used in this and next experiments.

From the above experiments, it was found that when the bottle diameter went beyond about 5 cm the transmitted intensity (I_x) through water, soft drink and beer was very low. Therefore, in the next experiment, two pieces of steel plate were placed in parallel 4.5 cm apart to limit the measurement of large bottle to thickness of liquid not more than 4.5 cm as illustrated in figure 3.5. The liquid samples were water, ethanol (70%) and kerosene contained in six types of plastic bottles having diameters of 4.9, 5.1, 5.5, 6.1, 6.2 and 6.3 cm as shown in figure 3.4. The transmitted intensity (I_x) and I_0 were measured the same way as in the previous experiments.
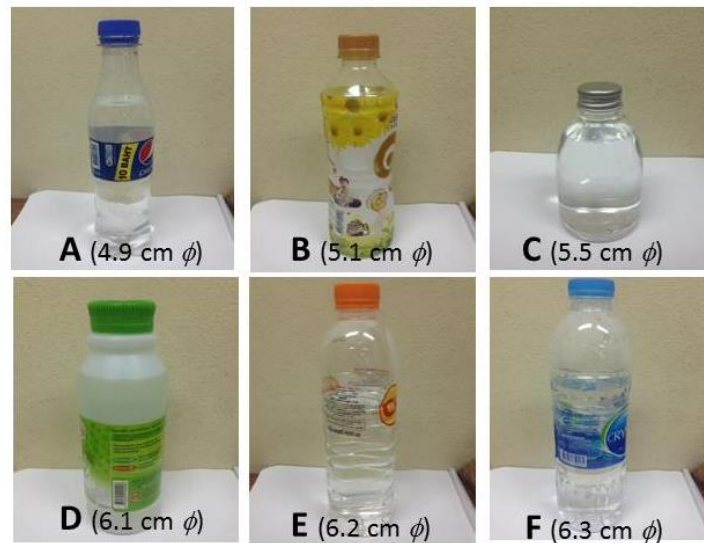
Figure 3.4 PET bottles having diameters of 4.9 to 6.3 cm
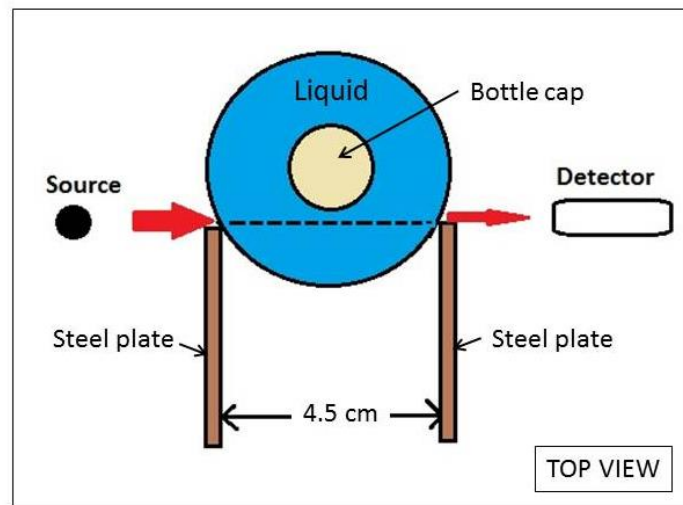
Figure 3.5 The Experiment set-up to limit the measurement thickness at 4.5 cm

3.3 Effect of bottle thickness

A 3.76 cm diameter PET bottle having thickness of 0.08 cm was selected as the liquid container. Plastic sheet with a thickness of 0.026 cm was inserted inside the liquid bottle one after the other to investigate the effect of plastic thickness on the obtained linear attenuation coefficient. Liquid samples were water, ethanol (70%) and kerosene. The obtained I_0 and I_x were then used to calculate the linear

attenuation coefficient of liquid at each plastic thickness. It should be noted that liquid thickness at each total plastic thickness was obtained from the difference of outside diameter of the bottle and the total thickness of plastic.
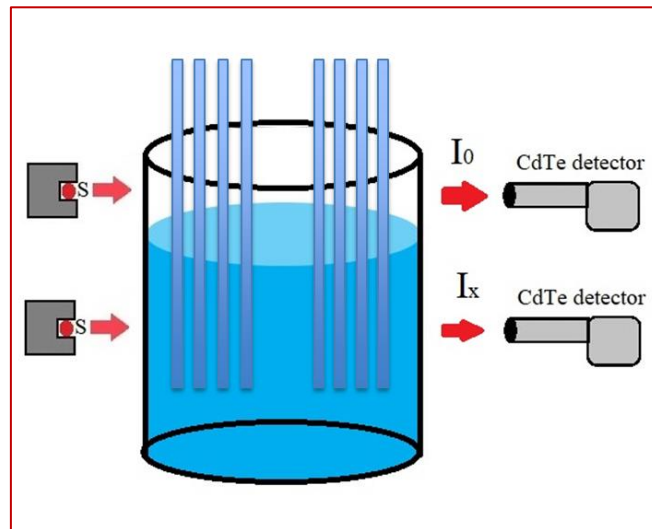
Figure 3.6 Experimental setup to investigate the effect of bottle thickness on the obtained linear attenuation coefficient of liquid

3.4 Effect of bottle types

There are various beverage products contained in different types of bottle such as plastic, glass and can. The obtained linear attenuation coefficient of liquid should be independent of the bottle type. Therefore, the purpose of this experiment was to investigate whether the bottle type would have effect on the obtained linear attenuation coefficient of liquid.

Types of bottle:
Polyethylene Terephthalate (PET) and High-density polyethylene (HDPE) [22]

Polyethylene Terephthalate sometimes absorbs odors and flavors from foods and drinks that are stored in them. Items made from this plastic are commonly recycled. PET(E) plastic is used to make many common household items like beverage bottles, medicine jars, rope, clothing and carpet fiber. High-Density

Polyethylene products are very safe and are not known to transmit any chemicals into foods or drinks. HDPE products are commonly recycled. Items made from this plastic include containers for milk, motor oil, shampoos and conditioners, soap bottles, detergents, and bleaches.
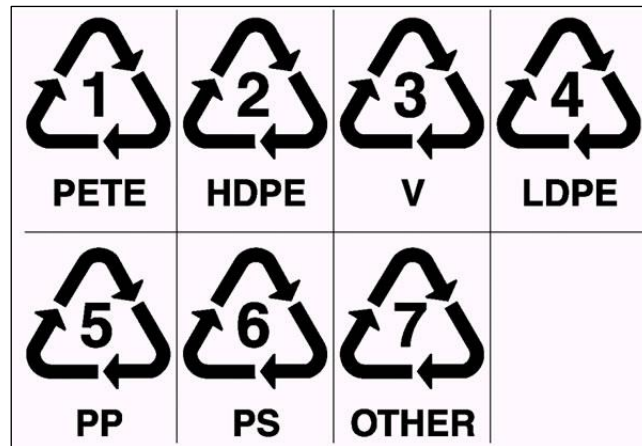
Figure 3.7 The Society of the Plastics Industry (SPI) symbols. [23]

Other types of plastic are showed in figure 3.7. Manufacturers place an SPI code, or number, on each plastic product, usually molded into the bottom. This guide provides a basic outline of the different plastic types associated with each code number.

Soda-lime glass[24]

For every drinking glass is soda-lime glass. Soda-lime glass is the most commonly available glass and contains both sodium and calcium. This type of glass is used for windows in buildings, bottles and jars. Composition of soda-lime glass is shown in Table 3.1

Table 3.1 Composition of soda-lime glass[24]

SiO_2	72.60%
Na_2O	13.90%
CaO	8.40%
MgO	3.90%
Al_2O_3	1.10%
K_2O	0.60%
SO_3	0.20%
Fe_2O_3	0.11%

Aluminum and steel cans[25]

There are two types of beverage cans. Major metal materials are aluminum and steel. Major cans are classified into two types: 3-piece cans consisting of three components of (1) a bottom lid, (2) a cylindrical body and (3) a top lid (a lid with a lip [an opening] for a beverage can), and 2-piece cans consisting of two components of (1) a body integrated with a bottom lid and (2) a lid with a lip (an opening). 2-Piece cans made from aluminum and use for a soft drink, beer, tea or fruit juice while 3-piece cans made from steel and use for beverages with milk, coffee or tea.

This experiment studied the effect of bottle types including PET plastic bottles, HDPE plastic bottles, glass bottles, aluminum cans and steel cans on the obtained linear attenuation coefficients. The linear attenuation coefficient of bottle material was determined and used to estimate the bottle thickness without measurement of the I_0 but I_0 was obtained from equation 3.1.

For empty bottle or at the empty portion of the bottle, the bottle thickness can also be calculated from equation 3.1 below.

$$I_{0=}\,I_{Air}\,e^{-\mu_b \cdot x_b} \tag{3.1}$$

Where I_0 is transmitted intensity through the bottle with no liquid

I_{Air} is the photon intensity through the air

μ_b is linear attenuation coefficient of the bottle (cm^{-1})

x_b is bottle thickness (cm)
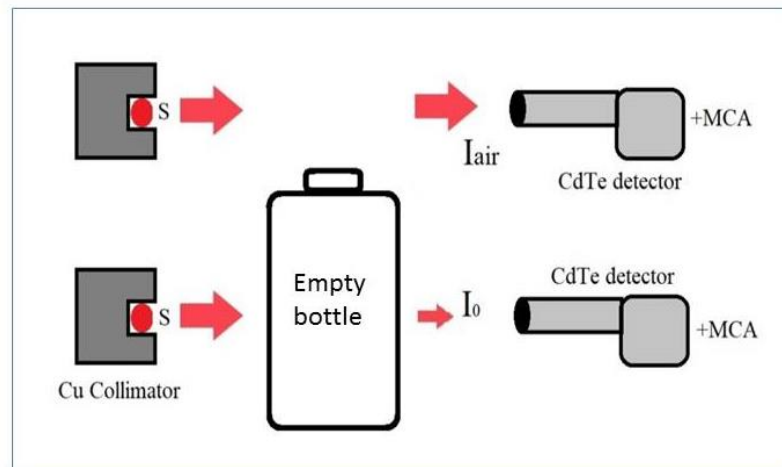
Figure 3.8 Experimental setup for determining of the linear attenuation coefficient of bottle (μ_{bottle})

3.4.1 Bottle with air portion inside

The linear attenuation coefficients of liquids in plastic bottles and glass bottles with air portion inside the bottles were calculated by using μ_{bottle} obtained from equation 3.1. Then liquid thickness was calculated by subtracting the bottle thickness from the bottle diameter. Finally, the linear attenuation coefficients of liquids were calculated by using equation 3.2

$$I_x = I_0 \, e^{-\mu x}$$

3.2

Where I_x is transmitted intensity through the bottle and liquid

I_0 is transmitted intensity through the bottle with no liquid

μ is linear attenuation coefficient of the liquid (cm^{-1})

X is liquid thickness (cm)

3.4.2 Bottle without air portion

Plastic bottle without air portion inside, I_0 could not be measured. The attenuation of x-rays by the bottle walls could be calculated from the linear attenuation coefficient of the plastic and its estimated thickness. It was expected that discrepancy of the estimated thickness from the actual value would have insignificant effect of the calculated linear attenuation coefficients of the liquids. This was because plastic had low linear attenuation coefficient as that of liquid and its thickness was small in comparison to liquid thickness. The estimated thickness of 0.02 and 0.05 cm were used in calculation of the linear attenuation of liquid contained in PET and HDPE bottles respectively. In contrast, for glass bottles, glass wall thickness was found to be in the range of 3 - 5 mm and had high linear attenuation coefficient. Estimation of glass thickness may cause large error in calculation of the linear attenuation coefficient of liquid contained in the bottle. Therefore, the glass thickness was measured using an ultrasonic thickness gauge when there was no air portion for measurement of I_0. The thicknesses of glass bottles measured by the ultrasonic thickness gauge and the x-ray transmission technique were tabulated in table 4.28. Finally, six types of glass bottles containing different kinds of liquid were selected for the test. The linear attenuation coefficients of liquids contained the glass bottles were compared with those obtained from other kinds of bottle.

For metal cans like aluminum and steel cans. The linear attenuation coefficients were so high in comparison with those of liquids. The linear attenuation coefficients of aluminum cans and steel cans were determined and used for calculation of I_0. Fortunately, thicknesses of aluminum and steel cans were found to be about 0.01 and 0.02 cm respectively which made calculation of attenuation by the aluminum and steel walls simpler.

Various kinds of commercial Liquid in PET, HDPE and glass bottles as well as aluminum and steel cans were tested using the above mentioned procedures including drinking water, orange juice, milk, green tea and coffee. The results are presented in Chapter 4.

Figure 3.9 Ultrasonic thickness gauge model IPX -251S

CHAPTER IV

RESULTS AND DISCUSSION

The experiments was carried out by measurement of the transmitted intensity of x-rays and gamma-rays through various kinds of liquid contained in different types of bottles with varying materials, thicknesses and diameters. The CdTe detector gave good energy resolution in measurement of the U L x-rays emitted from ^{238}Pu source at 13.6, 17.2 and 20.1 keV. The transmitted x-ray spectra through 3 kinds of liquid contained in plastic bottles is shown in Figure 4.1.
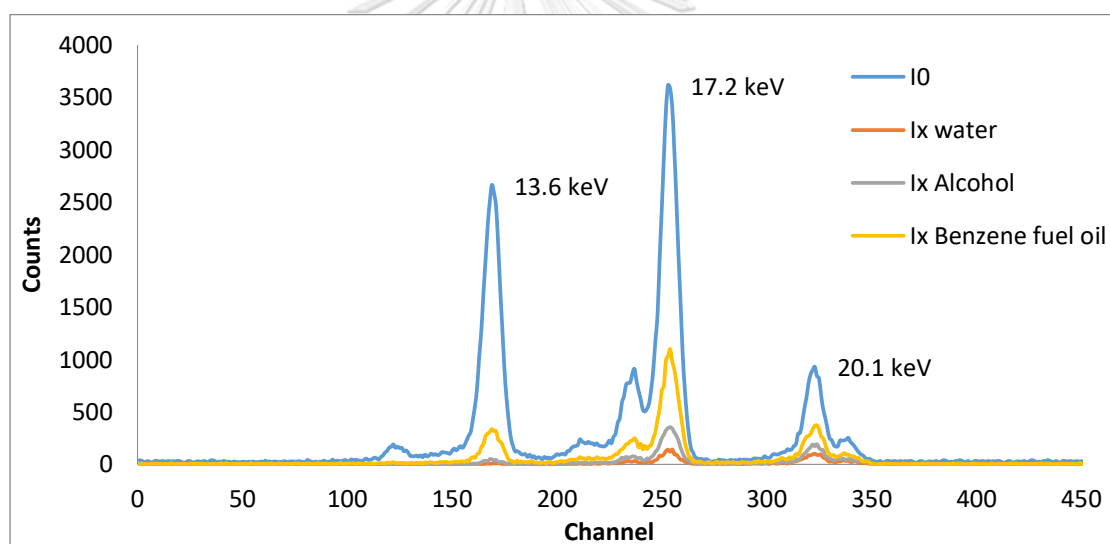
Figure 4.1 Transmitted x-ray spectra from ^{238}Pu source through water, alcohol and fuel oil

The primary results showed that transmitted intensity through water, alcohol and fuel oil were very different at this low energy range which indicated potential use of this proposed technique for screening liquid at airports. The linear attenuation coefficients of liquids calculated by using the NIST mass attenuation coefficient table and the values obtained from this preliminary experiment are shown in table 4.1 and 4.2. Discrepancies of the values obtained in the experiment from the calculated values are mainly due to interferences by neighboring x-ray peaks as can be seen in Figure 4.1 particularly at 17.2 and 20.1 keV peaks.

Table 4.1 Comparison of the linear attenuation coefficients of liquids at 13.6 and 17.2 keV obtained from experiment and calculation

Type of liquids	Chemical formula	Linear attenuation coefficient (cm^{-1})			
		13.6 keV		17.2 keV	
		Experiment	Calculation	Experiment	Calculation
Water	H_2O	2.2905	2.2838	1.1078	1.2779
Glycerin	$C_3H_8O_3$	2.0231	2.2453	1.1252	1.2531
H_2O_2 (12%)	H_2O_2(12%)+ H_2O(88%)	2.3910	2.4209	1.1896	1.3532
H_2O_2 (18%)	H_2O_2(18%)+ H_2O(82%)	2.3749	2.4900	1.1990	1.3911
Ethanol (95%)	C_2H_5OH(95%) +H_2O(5%)	1.2139	1.2202	0.6602	0.6883
Acetone	C_3H_6O	1.0273	1.1233	0.5580	0.6304
Methanol (70%)	CH_3OH(70%) +H_2O(30%)	1.2416	1.6084	0.6680	0.9031
Alcohol (70%)	C_2H_5OH(70%) +H_2O(30%)	1.4386	1.4782	0.7675	0.8315
Kerosene		0.7170	-	0.4240	-
Diesel		0.7415	-	0.4308	-
Gasohol 95		0.7049	-	0.4114	-
Gasohol E85		1.0304	-	0.5708	-
Gasohol E20		0.7812	-	0.4459	-
Nitromethane	CH_3NO_2	-	2.2399	-	1.2387
Nitroglycerine	$CHONO_2(CH2 ONO_2)_2$	-	3.3695	-	1.8557
Triacetone triperoxide TATP	$C_9H_{18}O_6$	-	1.6582	-	0.9246

Table 4.1 (continued) Comparison of the linear attenuation coefficients of liquids at 13.6 and 17.2 keV obtained from experiment and calculation

Type of liquids	Chemical formula	Linear attenuation coefficient (cm^{-1})			
		13.6 keV		17.2 keV	
		Experiment	Calculation	Experiment	Calculation
Hexamethylene triperoxide diamine HMTD	$C_6H_{12}O_6N_2$	-	1.3567	-	0.7518
Methyl ethyl ketone peroxide MEKP	$C_8H_{18}O_6$	-	1.6901	-	0.9432
Gasoline	C_7H_{16}	-	0.7559	-	0.4348
Alcohol	C_2H_5OH	-	1.1744	-	0.6629
H_2O_2 (100%)	H_2O_2	-	3.4698	-	1.9256
Ethanol (100%)	C_2H_5OH	-	1.1744	-	0.6629
Methanol (100%)	CH_3OH	-	1.3623	-	0.7664

Table 4.2 Comparison of the linear attenuation coefficients of liquids at 20.1 and 43.5 keV obtained from experiment and calculation

Type of liquids	Chemical formula	Linear attenuation coefficient (cm^{-1})			
		20.1 keV		43.5 keV	
		Experiment	Calculation	Experiment	Calculation
Water	H_2O	0.7324	0.8883	0.2377	0.2440
Glycerin	$C_3H_8O_3$	0.7649	0.8853	0.2896	0.2898
H_2O_2 (12%)	$H_2O_2(12\%)+$ $H_2O(88\%)$	0.7866	0.9397	0.2570	0.2562
H_2O_2 (18%)	$H_2O_2(18\%)+$ $H_2O(82\%)$	0.7984	0.9656	0.2674	0.2623

Table 4.2 (continue) Linear attenuation coefficient of liquids by experiment and calculation at 20.1 and 4.35 keV.

Type of liquids	Chemical formula	Linear attenuation coefficient (cm^{-1})			
		20.1 keV		43.5 keV	
		Experiment	Calculation	Experiment	Calculation
Ethanol (95%)	$C_2H_5OH(95\%)$ $+H_2O(5\%)$	0.4605	0.4951	0.1896	0.1840
Acetone	C_3H_6O	0.3955	0.4557	0.1800	0.1784
Methanol (70%)	$CH_3OH(70\%)$ $+H_2O(30\%)$	0.4623	0.6372	0.1848	0.2024
Ethanol (70%)	$C_2H_5OH(70\%)$ $+H_2O(30\%)$	0.5209	0.5912	0.2046	0.2004
Kerosene		0.3186	-	0.1821	-
Diesel		0.3229	-	0.1725	-
Gasohol 95		0.3069	-	0.1678	-
Gasohol E85		0.4021	-	0.1937	-
Gasohol E20		0.3316	-	0.1762	-
Nitromethane	CH_3NO_2	-	0.8624	-	0.2567
Nitroglycerine	$CHONO_2(CH2 ONO_2)_2$	-	1.2828	-	0.3570
Triacetone triperoxide TATP TATP	$C_9H_{18}O_6$	-	0.6568	-	0.2264
Hexamethylene triperoxide diamine HMTD	$C_6H_{12}O_6N_2$	-	0.5278	-	0.1684
Methyl ethyl ketone peroxide MEKP	$C_8H_{18}O_6$	-	0.6692	-	0.2278
Gasoline	C_7H_{16}	-	0.3312	-	0.1731

Table 4.2 (continued) Comparison of the linear attenuation coefficients of liquids at 20.1 and 43.5 keV obtained from experiment and calculation

Type of liquids	Chemical formula	Linear attenuation coefficient (cm^{-1})			
		20.1 keV		43.5 keV	
		Experiment	Calculation	Experiment	Calculation
Alcohol	C_2H_5OH	-	0.4780	-	0.1812
H_2O_2 (100%)	H_2O_2	-	1.3281	-	0.3431
Ethanol (100%)	C_2H_5OH	-	0.4780	-	0.1812
Methanol (100%)	CH_3OH	-	0.5453	-	0.1861

4.1 Effect of x-ray energy on the obtained μ

The linear attenuation coefficient (μ) is a basic parameter to identify matter. The total mass attenuation coefficient is sum of the product of mass attenuation coefficient and weight fraction of all elements as in equation 2.7. Theoretically, the attenuation coefficient is high at low x-ray energy and decreases with increasing of x-ray energy. The mass attenuation coefficient (μ/ρ) of some elements from the NIST is illustrated in Figure 4.2.
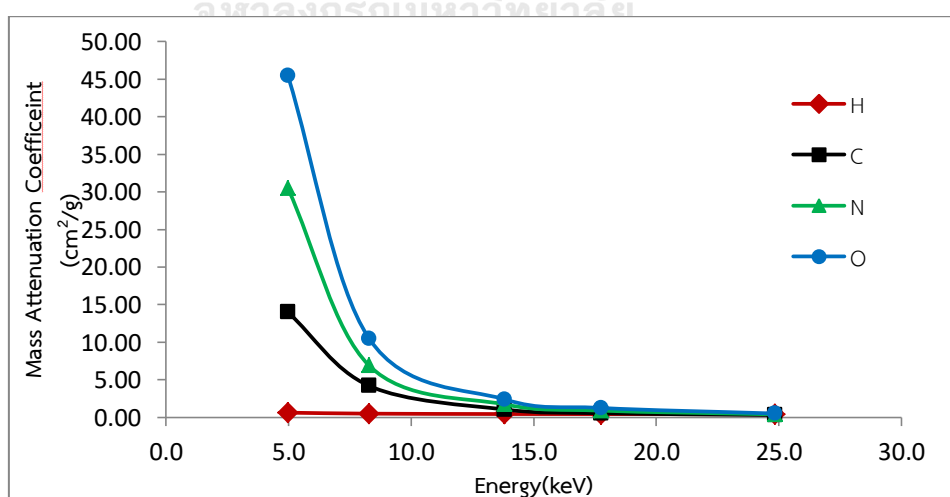
Figure 4.2 Mass attenuation coefficients (cm^2/g) of some elements from the NIST

The transmitted intensity (I_x) of x-rays and gamma-rays from [238]Pu, [241]Am and [57]Co radioisotope sources through various kinds of liquid samples contained in 3.1 cm diameter PET bottles were measured. The results are tabulated in Table 4.3. It should be noticed that 13.6 keV x-ray almost cannot penetrate water and soft drink even the bottle is rather small in diameter.

Table 4.3 Showing the transmitted intensities of x-rays and gamma-rays through various kinds of liquids contained in 3.1 cm diameter PET bottles

Types of liquid	I_0 and I_x through various kinds of liquid at different energies				
	13.6 keV	17.2 keV	20.1 keV	59.5 keV	122 keV
I_0	129487	261265	63812	135346	20089
I_X Drinking water	274	9548	7673	74628	12305
I_X Soft Drink	186	8022	6664	71867	12288
I_X Ethanol (70%)	1717	24248	13119	80692	13217
I_X Kerosene	15704	72800	24525	86056	13792
I_X Diesel	13335	68620	23791	82803	13243
I_X Benzene 95	17836	83320	28670	88074	13861

The linear attenuation coefficients of the liquid samples were calculated and tabulated in Table 4.4.

Table 4.4 Showing the linear attenuation coefficients of liquids for x-rays and gamma-rays at different energies

Types of liquid	Linear attenuation coefficient(cm^{-1}) for each energy				
	13.6 keV	17.2 keV	20.1 keV	59.5 keV	122 keV
Drinking water	2.0665±0.0203	1.1105±0.0035	0.7108±0.0041	0.1998±0.0015	0.1645±0.0038
Soft Drink	2.1965±0.0246	1.1689±0.0038	0.7581±0.0043	0.2124±0.0015	0.1649±0.0038
Ethanol (70%)	1.4507±0.0082	0.7977±0.0023	0.5308±0.0032	0.1736±0.0015	0.1405±0.0038
Kerosene	0.7079±0.0028	0.4288±0.0024	0.3209±0.0025	0.1520±0.0015	0.1262±0.0037
Diesel	0.7628±0.0031	0.4486±0.0014	0.3311±0.0025	0.1649±0.0015	0.1398±0.0038
Benzene 95	0.6652±0.0027	0.3835±0.0013	0.2685±0.0024	0.1442±0.0015	0.1245±0.0037
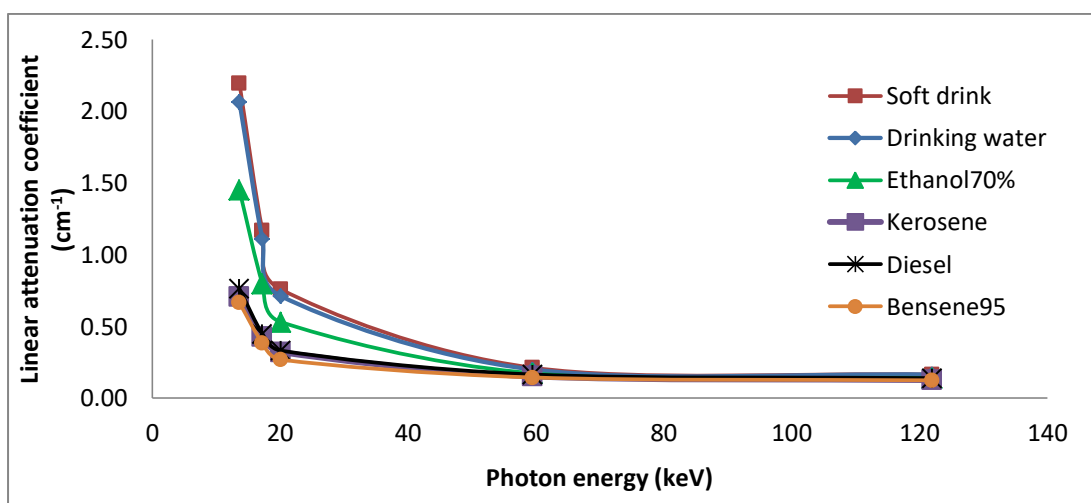
Figure 4.3 The obtained linear attenuation coefficients of liquids versus photon energy

The results demonstrate that the linear attenuation coefficients of all sample liquids are high at low energy and decrease rapidly from 10 to 20 keV. Difference of the linear attenuation coefficients of different kinds of liquid are also large at low energy and become closer toward higher energy. For example, the linear attenuation coefficients of drinking water, Ethanol (70%) and Benzene 95 at X-ray energy 13.6 keV are 2.0665±0.0203; 1.4507±0.0082 and 0.6652±0.0027 while at 122 keV are 0.1645±0.0038, 0.1405±0.0038 and 0.1245±0.0037 respectively.

4.2 Effect of bottle diameter on the obtained μ

The linear attenuation coefficients of drinking water, soft drink, beer, ethanol (70%), kerosene, Diesel, Benzene 95, gasohol 95, gasohol E20 and gasohol E85 fuel oil contained in PET bottles of different diameters were determined at different energies. The results are shown in the following table 4.5 to 4.12.

Table 4.5 The linear attenuation coefficients of drinking water contained in bottles having diameters 2.26 – 7.40 cm

Bottle diameter (cm)	Liquid thickness (cm)	Linear attenuation coefficient of drinking water (cm^{-1})				
		13.6 keV	17.2 keV	20.1 keV	60 keV	122 keV
2.26	1.96	2.1663	1.1602	0.7478	0.1999	0.1714
3.10	2.98	2.0665	1.1105	0.7108	0.1998	0.1645
3.33	3.17	2.1684	1.1363	0.7256	0.2015	0.1506
3.82	3.62	2.0495	1.1269	0.7279	0.2019	0.1594
4.96	4.84	*I$_X$ is low to calculate*	1.1191	0.7265	0.1986	0.1587
7.40	7.32		1.0470	0.6988	0.2303	0.1847
Average μ of drinking water		2.1127 ±0.0635	1.1167 ±0.0382	0.7229 ±0.0167	0.2053 ±0.0123	0.1649 ±0.0119

Table 4.6 The linear attenuation coefficients of soft drink contained in bottles having diameters 2.26 – 7.40 cm

Bottle diameter (cm)	Liquid thickness (cm)	Linear attenuation coefficient of soft drink (cm^{-1})				
		13.6 keV	17.2 keV	20.1 keV	60 keV	122 keV
2.26	1.96	2.2299	1.2122	0.8043	0.2146	0.1625
3.10	2.98	2.1965	1.1689	0.7581	0.2124	0.1649
3.33	3.17	2.0954	1.1655	0.7779	0.2123	0.1650
3.82	3.62	2.2022	1.1742	0.7623	0.2114	0.1661
4.96	4.84	I$_X$ is low to calculate	1.1452	0.7471	0.2065	0.1692
7.40	7.32		1.0301	0.7072	0.2032	0.1591
Average μ of soft drink		2.1810 ±0.0589	1.1494 ±0.0624	0.7595 ±0.0324	0.2101 ±0.0043	0.1645 ±0.0034

Table 4.7 The linear attenuation coefficients of beer contained in bottles having diameters 2.26 – 7.40 cm

Bottle diameter (cm)	Liquid thickness (cm)	Linear attenuation coefficient of beer (cm^{-1})				
		13.6 keV	17.2 keV	20.1 keV	60 keV	122 keV
2.26	1.96	2.3314	1.2847	0.8373	0.2067	0.1630
3.10	2.98	2.1082	1.1319	0.7329	0.2052	0.1693
3.33	3.17	2.0738	1.1233	0.7241	0.2045	0.1638
3.82	3.62	2.1486	1.1348	0.7302	0.2053	0.1670
4.96	4.84	I_X is low for calculation	1.1189	0.7209	0.2016	0.1587
7.40	7.32		1.1264	0.7191	0.1952	0.1573
Average μ of beer		2.1655 ±0.1148	1.1533 ±0.0646	0.7441 ±0.0460	0.2031 ±0.0042	0.1632 ±0.0046

Table 4.8 The linear attenuation coefficients of drinking ethanol(70%) contained in bottles having diameters 2.26 – 7.40 cm

Bottle diameter (cm)	Liquid thickness (cm)	Linear attenuation coefficient of ethanol(70%) (cm^{-1})				
		13.6 keV	17.2 keV	20.1 keV	60 keV	122 keV
2.26	1.96	1.4676	0.8093	0.5526	0.1734	0.1446
3.10	2.98	1.4507	0.7977	0.5308	0.1736	0.1405
3.33	3.17	1.4430	0.7919	0.5374	0.1734	0.1342
3.82	3.62	1.4727	0.7953	0.5390	0.1750	0.1442
4.96	4.84	1.4467	0.8106	0.5428	0.1727	0.1456
7.40	7.32	I_X is too low for calculation	0.7927	0.5324	0.1674	0.1382
Average μ of ethanol(70%)		1.4561 ±0.0132	0.7996 ±0.0083	0.5392 ±0.0079	0.1726 ±0.0026	0.1412 ±0.0044

Table 4.9 The linear attenuation coefficients of kerosene contained in bottles having diameters 2.26 – 7.40 cm

Bottle diameter (cm)	Liquid thickness (cm)	Linear attenuation coefficient of kerosene (cm^{-1})				
		13.6 keV	17.2 keV	20.1 keV	60 keV	122 keV
2.26	1.96	0.7263	0.4522	0.3469	0.1490	0.1310
3.10	2.98	0.7079	0.4288	0.3209	0.1520	0.1262
3.33	3.17	0.7035	0.4331	0.3266	0.1517	0.1234
3.82	3.62	0.7099	0.4344	0.3249	0.1511	0.1277
4.96	4.84	0.7145	0.4261	0.3163	0.1499	0.1248
7.40	7.32	0.7348	0.4405	0.3280	0.1431	0.1179
Average μ of kerosene		0.7161 ±0.0120	0.4359 ±0.0094	0.3273 ±0.0150	0.1495 ±0.0033	0.1252 ±0.0044

Table 4.10 The linear attenuation coefficients of diesel fuel oil contained in bottles having diameters 2.26 – 7.40 cm

Bottle diameter (cm)	Liquid thickness (cm)	Linear attenuation coefficient of diesel (cm^{-1})				
		13.6 keV	17.2 keV	20.1 keV	60 keV	122 keV
2.26	1.96	0.7768	0.4702	0.3499	0.1612	0.1505
3.10	2.98	0.7628	0.4486	0.3311	0.1649	0.1398
3.33	3.17	0.7480	0.4440	0.3207	0.1614	0.1369
3.82	3.62	0.7612	0.4524	0.3297	0.1625	0.1397
4.96	4.84	0.7558	0.4441	0.3229	0.1568	0.1342
7.40	7.32	0.7188	0.4233	0.3110	0.1552	0.1328
Average μ of diesel		0.7539 ±0.0196	0.4471 ±0.0152	0.3275 ±0.0131	0.1603 ±0.0036	0.1390 ±0.0063

Table 4.11 The linear attenuation coefficients of benzene95 fuel oil contained in bottles having diameters 2.26 – 7.40 cm

Bottle diameter (cm)	Liquid thickness (cm)	Linear attenuation coefficient of bensene95 (cm^{-1})				
		13.6 keV	17.2 keV	20.1 keV	60 keV	122 keV
2.26	1.96	0.6589	0.3863	0.2724	0.1435	0.1278
3.10	2.98	0.6652	0.3835	0.2685	0.1442	0.1245
3.33	3.17	0.6537	0.3859	0.2830	0.1422	0.1195
3.82	3.62	0.6647	0.3939	0.2784	0.1457	0.1246
4.96	4.84	0.6523	0.3864	0.2714	0.1378	0.1196
7.40	7.32	0.6286	0.3676	0.2694	0.1391	0.1180
Average μ of Bensene95		0.6539 ±0.0135	0.3839 ±0.0087	0.2738 ±0.0057	0.1421 ±0.0031	0.1223 ±0.0039

Table 4.12 The linear attenuation coefficients of gasohol95 fuel oil contained in bottles having diameters 2.26 – 7.40 cm

Bottle diameter (cm)	Liquid thickness (cm)	Linear attenuation coefficient of gasohol95 (cm^{-1})				
		13.6 keV	17.2 keV	20.1 keV	60 keV	122 keV
2.26	1.96	0.7293	0.4207	0.2946	0.1449	0.1147
3.10	2.98	0.7089	0.4104	0.2903	0.1466	0.1172
3.33	3.17	0.7086	0.4067	0.2907	0.1510	0.1228
3.82	3.62	0.7088	0.4152	0.2916	0.1469	0.1094
4.96	4.84	0.7075	0.4134	0.2928	0.1449	0.1157
7.40	7.32	0.6893	0.3950	0.2890	0.1486	0.1215
Average μ of Gasohol95		0.7087 ±0.0127	0.4102 ±0.0088	0.2915 ±0.0020	0.1471 ±0.0024	0.1169 ±0.0049

Table 4.13 The linear attenuation coefficients of gasohol E20 fuel oil contained in bottles having diameters 2.26 – 7.40 cm

Bottle diameter (cm)	Liquid thickness (cm)	Linear attenuation coefficient of gasoholE20 (cm^{-1})				
		13.6 keV	17.2 keV	20.1 keV	60 keV	122 keV
2.26	1.96	0.7664	0.4445	0.3074	0.1500	0.1290
3.10	2.98	0.7628	0.4346	0.2991	0.1477	0.1152
3.33	3.17	0.7550	0.4327	0.3022	0.1512	0.1123
3.82	3.62	0.7664	0.4373	0.3000	0.1450	0.1166
4.96	4.84	0.7524	0.4343	0.2998	0.1456	0.1140
7.40	7.32	0.7342	0.4205	0.2974	0.1504	0.1235
Average μ of gasohol E20		0.7562 ±0.0122	0.4340 ±0.0078	0.3010 ±0.0035	0.1483 ±0.0026	0.1184 ±0.0064

Table 4.14 The linear attenuation coefficients of gasohol E85 fuel oil contained in bottles having diameters 2.26 – 7.40 cm

Bottle diameter (cm)	Liquid thickness (cm)	Linear attenuation coefficient of gasoholE85 (cm^{-1})				
		13.6 keV	17.2 keV	20.1 keV	60 keV	122 keV
2.26	1.96	1.0131	0.5644	0.3804	0.1632	0.1226
3.10	2.98	1.0042	0.5528	0.3693	0.1566	0.1258
3.33	3.17	0.9971	0.5515	0.3783	0.1582	0.1259
3.82	3.62	0.9953	0.5580	0.3776	0.1560	0.1177
4.96	4.84	0.9993	0.5565	0.3774	0.1557	0.1210
7.40	7.32	0.9382	0.5248	0.3711	0.1565	0.1277
Average μ of gasohol E85		0.9912 ±0.0268	0.5513 ±0.0138	0.3757 ±0.0044	0.1577 ±0.0028	0.1234 ±0.0037

The results show that the linear attenuation coefficients of the same kind of liquid obtained from different bottle sizes are very close. But when the bottle diameter becomes larger than about 5 cm, the transmitted intensity of the water-based liquids such as drinking water, soft drink, and beer was too low to calculate the linear attenuation coefficient at 13.6 keV. However, higher energy such as 20.1 keV can penetrate the water-based liquids but the linear attenuation coefficients become closer. The linear attenuation coefficient of liquids at 13.6 keV and 20.1 keV contained in various bottle diameters are presented in Figure 4.4 and Figure 4.5.
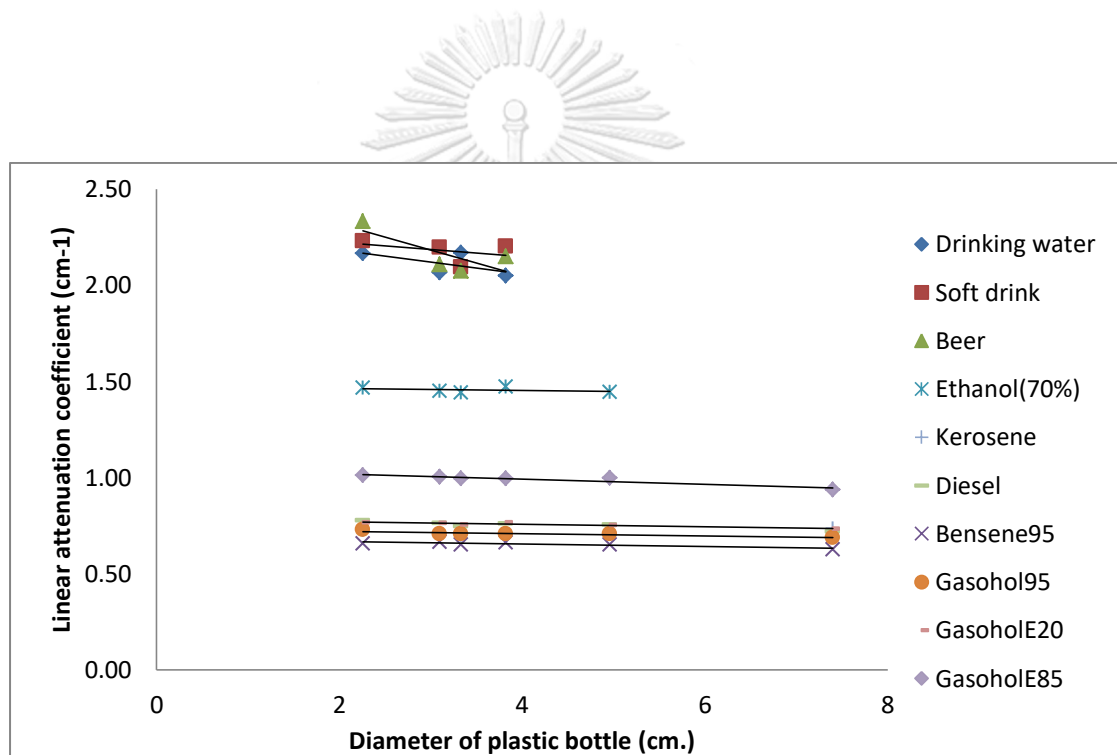
Figure 4.4 The linear attenuation coefficients of liquids contained in various bottle diameters for 13.6 keV x-rays
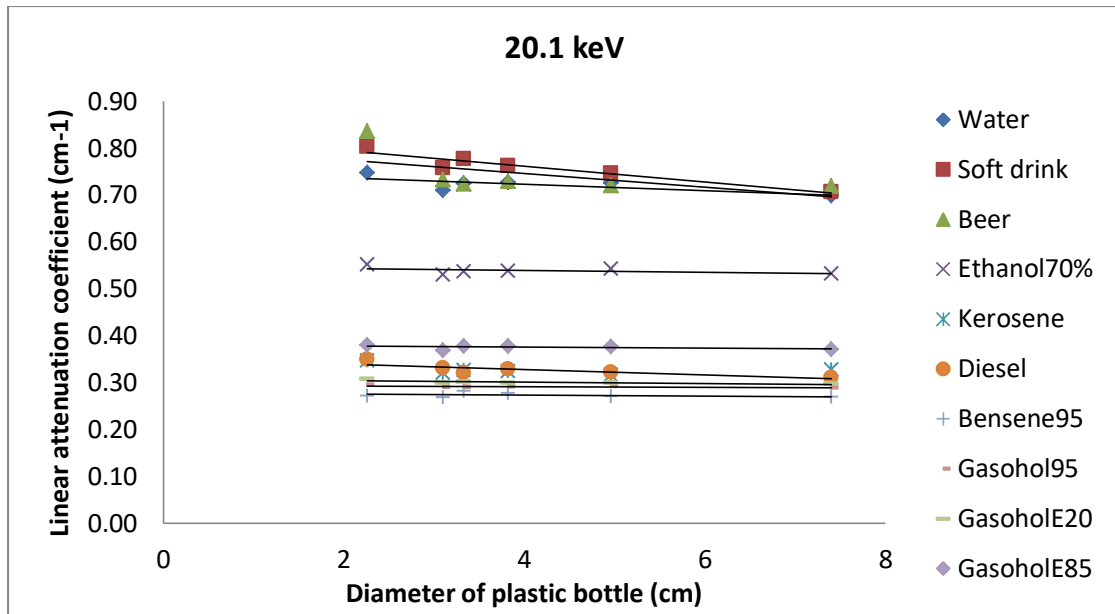
Figure 4.5 The linear attenuation coefficients of liquids contained in various bottle diameters for 20.1 keV x-rays

When liquid thickness was fixed to 4.5 cm, the linear attenuation coefficients of water, ethanol (70%) and kerosene contained in different types of bottles were found to be close to the values obtained earlier. However, they tend to gradually increase with increasing of the bottle diameter which most probably caused by curvature and thickness of the bottles. For example, the linear attenuation coefficient of water in bottle A (4.9 cm ϕ) and bottle F (6.3 cm ϕ) at 17.2 keV are 1.1773 and 1.2184 cm^{-1} respectively. But the average linear attenuation coefficients of water, ethanol (70%) and kerosene still have large differences. For example, the average linear attenuation coefficients of water, ethanol (70%) and kerosene at 17.2 keV are 1.2008±0.0167, 0.8374±0.0196 and 0.4769±0.0139 respectively.

Table 4.15 The linear attenuation coefficients of water contained in large bottles but liquid thickness was fixed at 4.5 cm

Type of bottle	Linear attenuation coefficient (cm^{-1})			
	13.6 keV	17.2 keV	20.1 keV	43.5 keV
A (4.9 cm ϕ)	Ix water is too low for calculation	1.1773	0.7720	0.2452
B (5.1 cm ϕ)		1.1917	0.7762	0.2558
C (5.5 cm ϕ)		1.1923	0.7826	0.2651
D (6.1 cm ϕ)		1.2055	0.8010	0.2860
E (6.2 cm ϕ)		1.2195	0.8102	0.2911
F (6.3 cm ϕ)		1.2184	0.8083	0.2812
Average μ of water		**1.2008 ±0.0167**	**0.7917 ±0.0168**	**0.2707 ±0.0183**

Table 4.16 The linear attenuation coefficients of ethanol(70%) contained in large bottles but liquid thickness was fixed at 4.5 cm

Type of bottle	Linear attenuation coefficient (cm^{-1})			
	13.6 keV	17.2 keV	20.1 keV	43.5 keV
A (4.9 cm ϕ)	1.5162	0.8146	0.5494	0.2263
B (5.1 cm ϕ)	1.5921	0.8402	0.5735	0.2180
C (5.5 cm ϕ)	1.5662	0.8227	0.5645	0.2335
D (6.1 cm ϕ)	1.5116	0.8298	0.5686	0.2247
E (6.2 cm ϕ)	1.5688	0.8480	0.5739	0.2312
F (6.3 cm ϕ)	1.5767	0.8690	0.5829	0.2307
Average μ of ethanol(70%)	**1.5553 ±0.0333**	**0.8374 ±0.0196**	**0.5688 ±0.0113**	**0.2274 ±0.0057**

Table 4.17 The linear attenuation coefficients of kerosene contained in large bottles but liquid thickness was fixed at 4.5 cm

Type of bottle	Linear attenuation coefficient (cm^{-1})			
	13.6 keV	17.2 keV	20.1 keV	43.5 keV
A (4.9 cm ϕ)	0.7697	0.4502	0.3277	0.1807
B (5.1 cm ϕ)	0.8353	0.4825	0.3465	0.1828
C (5.5 cm ϕ)	0.8109	0.4763	0.3520	0.2077
D (6.1 cm ϕ)	0.8142	0.4816	0.3521	0.1930
E (6.2 cm ϕ)	0.8178	0.4798	0.3524	0.1915
F (6.3 cm ϕ)	0.8321	0.4908	0.3567	0.2116
Average μ of kerosene	0.8133 ±0.0235	0.4769 ±0.0139	0.3479 ±0.0104	0.1945 ±0.0127

4.3 Effect of bottle thickness on the obtained μ

Since the bottles not only have difference in diameter but also the thickness. For a thin plastic bottles like drinking water bottles or soft drink bottles, the thickness can be ignored because the linear attenuation coefficients of plastics fall in the same range as the linear attenuation coefficients of liquids. Conversely, thick bottles may affect the linear attenuation coefficients of liquids if it is not taken into account in measurement or in calculation. The transmitted intensity and linear attenuation coefficients of water, ethanol (70%) and kerosene at various plastic thicknesses are shown in table 4.18.

Table 4.18 Transmitted intensity and the linear attenuation coefficients of water in various plastic thicknesses

Thickness of plastic (cm)	Transmitted Intensity			Linear attenuation coefficient (cm^{-1}) of water		
	13.6 keV	17.2 keV	20.1 keV	13.6 keV	17.2 keV	20.1 keV
0.160	34	10184	10729		1.1515	0.7609
0.212	96	9942	10878		1.1589	0.7562
0.264	134	10224	10477	I$_X$ is too low for calculation	1.1529	0.7704
0.316	161	9972	10719		1.1612	0.7661
0.368	99	10151	10964		1.1569	0.7604
0.420	108	10053	10984		1.1629	0.7590
Average µ of water					1.1574 ±0.0045	0.7622 ±0.0051

Table 4.19 Transmitted intensity and the linear attenuation coefficients of ethanol(70%) in various plastic thicknesses

Thickness of plastic (cm)	Transmitted Intensity			Linear attenuation coefficient (cm^{-1}) of ethanol (70%)		
	13.6 keV	17.2 keV	20.1 keV	13.6 keV	17.2 keV	20.1 keV
0.160	1645	33246	22684	1.4813	0.8076	0.5432
0.212	1508	32065	22105	1.5009	0.8133	0.5469
0.264	1566	32509	22259	1.4811	0.8061	0.5445
0.316	1504	32339	21910	1.4880	0.8029	0.5484
0.368	1313	31402	21618	1.5211	0.8075	0.5504
0.420	1557	31342	21526	1.4614	0.8053	0.5474
Average µ of ethanol(70%)				1.4890 ±0.0203	0.8070 ±0.0035	0.5468 ±0.0026

Table 4.20 Transmitted intensity and the linear attenuation coefficients of kerosene in various plastic thicknesses

Thickness of plastic (cm)	Transmitted Intensity			Linear attenuation coefficient (cm^{-1}) of kerosene		
	13.6 keV	17.2 keV	20.1 keV	13.6 keV	17.2 keV	20.1 keV
0.160	24279	126381	51075	0.6988	0.4194	0.3073
0.212	22251	122536	49961	0.7065	0.4176	0.3063
0.264	21065	118266	48908	0.7020	0.4190	0.3085
0.316	19703	115354	48382	0.7046	0.4157	0.3072
0.368	18385	111074	46948	0.7045	0.4166	0.3104
0.420	17448	109461	46952	0.7015	0.4120	0.3022
Average μ of kerosene				0.7030 ±0.0027	0.4167 ±0.0027	0.3070 ±0.0028

The results show that when thickness of the bottle increases from 0.16 to 0.42 cm, the transmitted intensity decreases accordingly but the linear attenuation coefficient of water is still statistically constant. This means, for plastic bottles, the thickness does not have to be accurately known. Estimation of thickness should be enough for satisfactorily determining the linear attenuation coefficient of liquid. When plastic bottles, having diameter of 3.9 cm and thickness of 0.06 cm, filled with different kinds of liquids were tested in determining the linear attenuation coefficients of liquids by using estimated thickness the obtained value for water based liquids were statistically constant. However, the values of alcohol and fuel oil group tended to have little decrease when the estimated thickness went far beyond the actual value (as shown in Table 4.21 and Figure 4.6). This is mainly because the linear attenuation coefficients of plastic are greater than those of alcohol and fuel oil. In practice, user can actually estimate the bottle thickness from his/her experience or from the bottle data base. By using a Vernier caliper, the average thickness of commercial PET and HDPE plastic bottles were found to be about 0.02 cm and 0.05 cm respectively.

Table 4.21 The linear attenuation coefficient of liquids obtained by using the estimated thickness of plastic bottles.

Types of liquid	Linear Atten. Coef. for estimate plastic thickness at 17.2 keV							
	0.02 cm	0.04 cm	0.06 cm	0.08 cm	0.10 cm	0.12 cm	0.20 cm	Standard deviation
Water	1.1064	1.1069	1.1073	1.1078	1.1082	1.1087	1.1106	±0.0014
Glycerin	1.1256	1.1261	1.1266	1.1272	1.1277	1.1283	1.1306	±0.0017
H_2O_2 (12%)	1.1889	1.1898	1.1906	1.1915	1.1924	1.1933	1.1970	±0.0027
H_2O_2 (18%)	1.1958	1.1967	1.1976	1.1985	1.1994	1.2004	1.2042	±0.0028
Ethanol (70%)	0.7784	0.7772	0.7759	0.7746	0.7733	0.7720	0.7666	±0.0039
Ethanol (95%)	0.6708	0.6689	0.6671	0.6653	0.6634	0.6615	0.6537	±0.0057
Methanol(70%)	0.6810	0.6792	0.6774	0.6756	0.6738	0.6719	0.6644	±0.0055
Acetone	0.5725	0.5701	0.5678	0.5654	0.5630	0.5606	0.5506	±0.0073
Kerosene	0.4404	0.4374	0.4343	0.4313	0.4282	0.4250	0.4121	±0.0094
Diesel	0.4502	0.4472	0.4442	0.4412	0.4381	0.4350	0.4224	±0.0092
Gasohol 95	0.4318	0.4288	0.4257	0.4226	0.4194	0.4162	0.4031	±0.0095
Gasohol E85	0.5875	0.5852	0.5830	0.5807	0.5784	0.5760	0.5664	±0.0070
Gasohol E20	0.4647	0.4618	0.4589	0.4559	0.4529	0.4499	0.4376	±0.0090
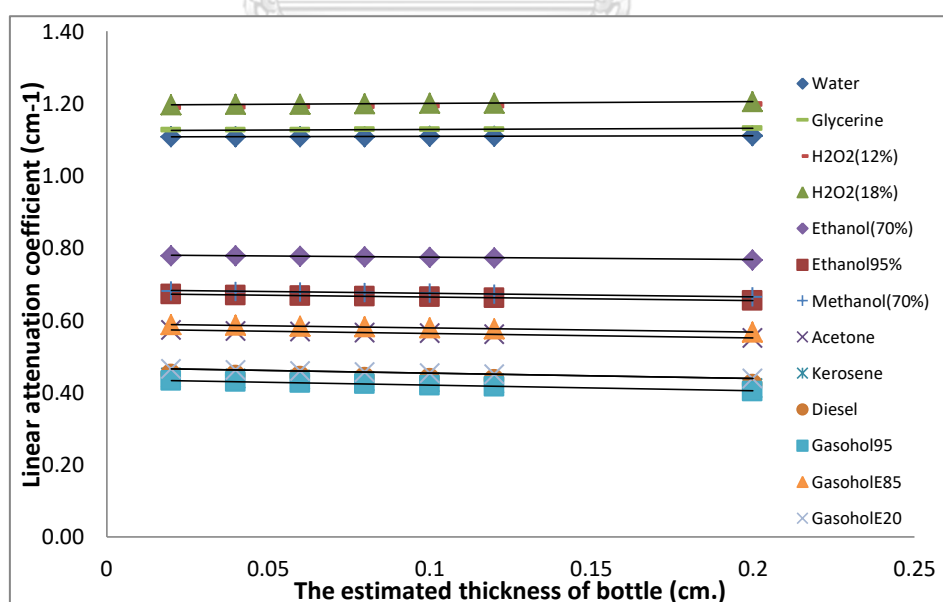
Figure 4.6 The linear attenuation coefficient of liquids obtained by using the estimated thickness of plastic bottles

4.4 Effect of bottle types on the obtained μ

The average linear attenuation coefficients of plastic bottles, glass bottles and metal cans obtained from this experiment are shown in Table 4.22 – 4.24.

Table 4.22 The average linear attenuation coefficients of plastic bottles

Types of plastic	Thickness (cm)	Average linear attenuation coefficient (cm^{-1})		
		13.6 keV	17.2 keV	20.1 keV
HDPE (shampoo)	0.050 - 0.073	1.6201±0.1093	0.8804±0.0513	0.5604±0.0306
HDPE (milk)	0.042 – 0.054	1.0890±0.1065	0.5333±0.0328	0.3778±0.0187
PET	0.024 – 0.050	2.3628±0.5720	1.1725±0.1610	0.5195±0.1424
Average μ$_{plastic}$		1.6906±0.3418	0.8621±0.0994	0.4859±0.0848

Table 4.23 The average linear attenuation coefficients of glass bottles

Types of glass	Average linear attenuation coefficient (cm^{-1}) of glass			
	13.6 keV	17.2 keV	20.1 keV	43.5 keV
Orange Juice		11.9265±0.0225	7.3157±0.0211	1.0791±0.1075
Wine		12.5804±0.0322	7.6838±0.1031	0.9574±0.0688
Mineral water	I$_x$ is too low for calculation	12.3928±0.0485	7.5391±0.0396	1.0543±0.0228
Beer1		12.1246±0.0675	7.6488±0.0532	1.1575±0.0100
Beer2		13.1448±0.1166	8.0135±0.0372	1.2196±0.0342
Average μ$_{glass}$		12.4338±0.0664	7.6402±0.0581	1.0936±0.0601

Table 4.24 The average linear attenuation coefficients of metal cans

Types of can	Average linear attenuation coefficient (cm^{-1}) of can			
	13.6 keV	17.2 keV	20.1 keV	43.5 keV
Aluminum can	30.8244 ±0.3237	15.3854 ±0.1679	9.6949 ±0.4472	1.3640 ±0.3914
Steel can	I_x is too low for calculation		145.2940 ±2.7782	18.4622 ±0.6844

The results show that average linear attenuations of PET and HDPE bottles are quite different from 1.1 to 2.4 cm^{-1} while the average value is about 1.7 cm^{-1} at 13.6 keV. However, the plastic bottle thickness only has little effect on the linear attenuation coefficient of liquid. This is because plastic is so thin in comparison to thickness of liquid and the linear attenuation coefficient is relatively low. The estimated thickness will give satisfactory result.

The glass bottles are thick and the linear attenuation of glass bottle is found to be very high. For example, at 17.2 keV the average value is 12.4338±0.0664 cm^{-1} while it is only 0.8621±0.0994 cm^{-1} for plastic bottles. The 13.6 keV x-rays cannot penetrate the glass bottles. Thus, thickness of glass bottle needs to be measured by some means. The values obtained by x-ray transmission technique and by ultrasonic thickness gauge are shown in Table 4.25.

Table 4.25 Comparison thicknesses of glass bottle measured by ultrasonic thickness gauge and by x-ray transmission technique

Types of glass	Thickness from UT (cm)	x-ray transmission technique (cm)	% difference
Bottle glass 1	0.4290±0.0004	0.4365±0.0270	1.748
Bottle glass 2	0.4050±0.0004	0.4048±0.0085	0.049
Bottle glass 3	0.3600±0.0004	0.3707±0.0196	2.972
Bottle glass 4	0.3740±0.0004	0.3683±0.0050	1.524
Bottle glass 5	0.3610±0.0004	0.3796±0.0173	5.152
Bottle glass 6	0.3500±0.0004	0.3674±0.0191	4.971

The results show that % different from ultrasonic thickness gauge and calculation is lower than 5%. Therefore, for the bottle with air gap inside can use ultrasonic thickness gauge or calculation by transmission technique.

4.4.1 Result of bottle with air portion

The linear attenuation coefficients of liquids contained in plastic bottles with air portion were calculated and presented in the following tables.

Table 4.26 The linear attenuation coefficients of liquids contained in 3.9 cm diameter PET bottle with air portion for measurement of I_0

Types of liquid	Linear attenuation coefficient (cm^{-1})			
	13.6 keV	17.2 keV	20.1 keV	43.5 keV
Water	too low I_X	1.1037±0.0027	0.7297±0.0026	0.2369±0.0060
Ethanol(95%)	1.2095±0.0045	0.6578±0.0012	0.4589±0.0016	0.1889±0.0056
H_2O_2(18%)	I_X low to cal.	1.1947±0.0032	0.7955±0.0029	0.2665±0.0062
Acetone	1.0236±0.0032	0.5559±0.0010	0.3941±0.0015	0.1793±0.0055
Kerosene	0.7148±0.0018	0.4227±0.0008	0.3176±0.0013	0.1815±0.0055
Diesel fuel oil	0.7388±0.0019	0.4292±0.0008	0.3217±0.0013	0.1719±0.0055
Methanol(70%)	1.2372±0.0048	0.6657±0.0012	0.4607±0.0016	0.1841±0.0055
H_2O_2(12%)	I_X low to cal.	1.1855±0.0031	0.7838±0.0028	0.2561±0.0061
Glycerin	2.0163±0.0208	1.1215±0.0028	0.7624±0.0027	0.2886±0.0063
Ethanol(70%)	1.4330±0.0070	0.7645±0.0014	0.5189±0.0018	0.2039±0.0057
Gasohol95	0.7023±0.0018	0.4099±0.0008	0.3058±0.0013	0.1672±0.0055
E85 fuel oil	1.0265±0.0032	0.5687±0.0010	0.4006±0.0015	0.1930±0.0055
E20 fuel oil	0.7784±0.0020	0.4443±0.0008	0.3304±0.0013	0.1494±0.0054

Table 4.27 Transmitted intensity ratio of liquids per water for bottle diameter 3.9 cm

Types of liquid	Ratio of I_X/I_{Xwater} at each energy		
	13.6 keV	17.2 keV	20.1 keV
Water		1	1
H_2O_2(12%)		0.7262±0.0080	0.8109±0.0110
H_2O_2(18%)		0.7072±0.0111	0.7809±0.0142
Glycerin		0.9285±0.0099	0.8718±0.0107
Ethanol(70%)		3.5706±0.0373	2.1745±0.0103
Methanol(70%)	I_X water is too low	5.2117±0.0545	2.7464±0.0104
Ethanol(95%)	for calculation	5.4219±0.0596	2.7727±0.0110
Kerosene		13.2538±0.2059	4.7713±0.0141
Diesel fuel oil		12.7613±0.1853	4.6574±0.0138
Gasohol95 fuel oil		13.7011±0.1562	4.9084±0.0114
E85 fuel oil		7.4898±0.0782	3.4404±0.0103
E20 fuel oil		12.0624±0.1294	4.5063±0.0107
Acetone		7.9397±0.0832	3.5247±0.0104

The results show that linear attenuation coefficients of liquids can be divided into 2 groups. The first group was water-based such as drinking water and H_2O_2 (12-18%). This group had a linear attenuation coefficient more than 1.1 cm^{-1} at 17.2 keV. The second group was a hazardous group as ethanol (70%), ethanol (95%), Methanol (70%), gasohol E85, kerosene and fuel oil which have a linear attenuation coefficient lower than 1.0 cm^{-1} at x-ray energy 17.2 keV.

Low energy x-ray at 13.6 keV has the highest linear attenuation coefficient and has large difference between elements but for a bottle diameter more than 3 cm linear attenuation coefficients for water-based liquids could not be calculated because water-based liquids had a high linear attenuation coefficient at low energy then the transmitted intensity could not penetrate through water-based liquids.

The ratio of the transmitted intensity of liquids per the transmitted intensity of water is used to make a clear difference between different kinds of liquid. The ratio of the bottle diameter 3.9 cm was shown in Figure 4.7 and Figure 4.8.

The bottles which diameter 3.9 cm has transmitted intensities of ethanol (70%) and gasohol 95 compared with water (I_{XL}/I_{XW}) are approximately 3.5 and 13.7 respectively at 17.2 keV. When the bottles become larger, the I_{XL}/I_{XW} values become higher at each energy peak. For example at diameter 4.5 cm. and 17.2 keV I_{XL}/I_{XW} values of ethanol (70%) and gasohol95 is 4.5 and 22.7 respectively. It should be noted that the transmitted intensity at 17.2 keV peak is only about 1.53 % for water contained in 3.9 cm diameter bottle but for ethanol (70%) and gasohol 95 are about 5.5 and 21.2 % respectively. It is of importance to note the differences of I_{XL}/I_{XW} values of various fuel oils decreases with increasing of a percentage of ethanol. The I_{XL}/I_{XW} value of ethanol is much lower than those of the fuel oils while diesel oil stays in between alcohol and gasohol 95. The experiment also shows that water-based liquids like a soft drink, fruit juice, syrup and saline solution have I_{XL}/I_{XW} values less than 1.0 due to absorption by sugar, salt, and other added substances.
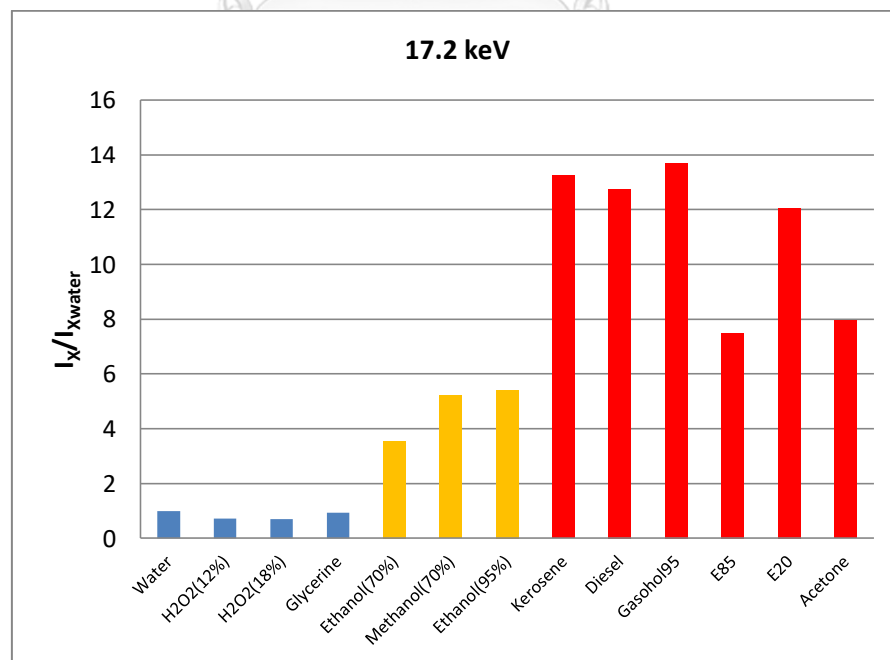
Figure 4.7 Ratio of I_{XL}/I_{XW} at 17.2 keV in bottle diameter 3.9cm
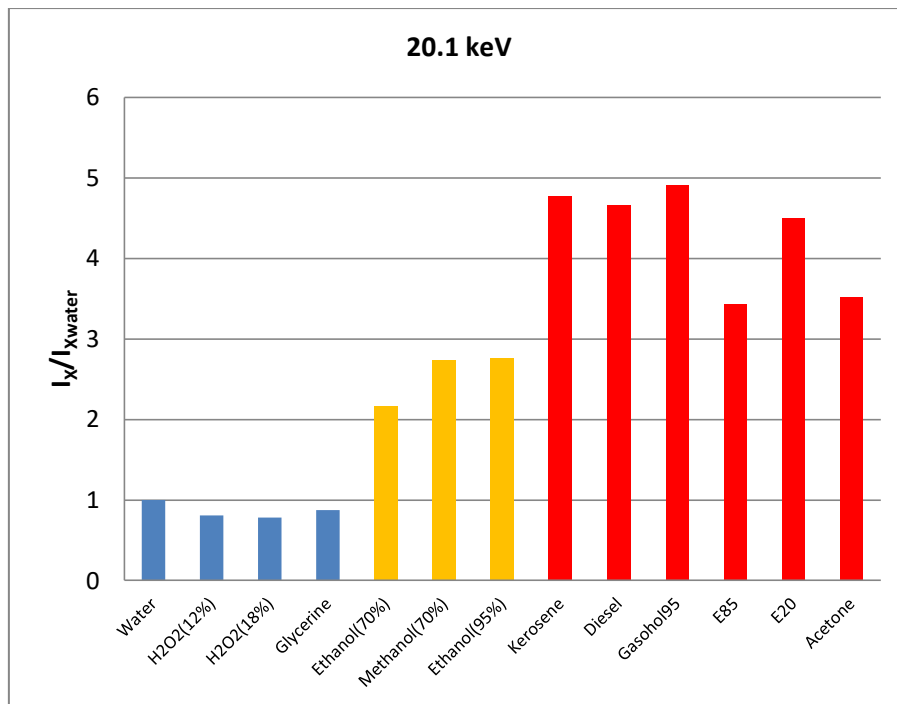
Figure 4.8 Ratio of I_{XL}/I_{XW} at 20.1 keV in bottle diameter 3.9cm

Water, H_2O_2 (18%), diesel, acetone, kerosene and ethanol (70%) were selected for measuring linear attenuation coefficient of liquids in the glass bottle with air inside and the results are shown in table 4.28.

Table 4.28 The linear attenuation coefficient of liquids in glass bottles

Types of liquid	Linear attenuation coefficient (cm^{-1})			
	13.6 keV	17.2 keV	20.1 keV	43.5 keV
Water	Ix is too low for calculation	Ix low to calculate	0.6033±0.0123	0.2222±0.0061
H_2O_2 (18%)			0.6673±0.0132	0.2576±0.0063
Diesel		0.4307±0.0063	0.3183±0.0049	0.1649±0.0052
Acetone		0.5318±0.0088	0.3861±0.0059	0.1555±0.0050
Kerosene		0.3984±0.0064	0.2949±0.0047	0.1551±0.0050
Ethanol (70%)		0.7806±0.0158	0.4721±0.0070	0.1819±0.0051

The Glass bottle has a high linear attenuation coefficient. Thus the intensity of low energy X-ray such as 13.7 keV cannot transmit and calculate the linear attenuation of liquids in the glass bottle. For 17.2 keV X-ray energy, a photon can transmit the glass but for water-based liquids, it cannot transmit through glass and liquids. In contrast, photon energy 17.2 keV can transmit the flammable liquids such-as ethanol or fuel oil in the glass bottle. Higher energy X-ray (20.1 and 43.5 keV) has a high penetration then linear attenuation coefficient can be calculated.

Theoretical, linear attenuation coefficient of the same liquid in other types of bottles must be the same value. Therefore, the linear attenuation coefficient of liquids contained in glass and plastic bottles were compared and shown in figure 4.9 and figure 4.10. The results show that the linear attenuation coefficients of liquids in plastic bottles were a little higher than in the glass bottles.   This was because the transmitted intensity of x-rays at energy was low. Higher x-ray energy may be better for the glass bottles with diameter around 5-6 cm but the intensity of 43.5 keV x-rays from ^{238}Pu was too low for this application.

20.2 keV

	Water	H2O2 18%	Diesel	Acetone	Kerosene	Ethanol70%
liquids in plastic	0.7303	0.7960	0.3220	0.3948	0.3179	0.5201
Liquids in glass	0.6033	0.6673	0.3183	0.3861	0.2949	0.4721
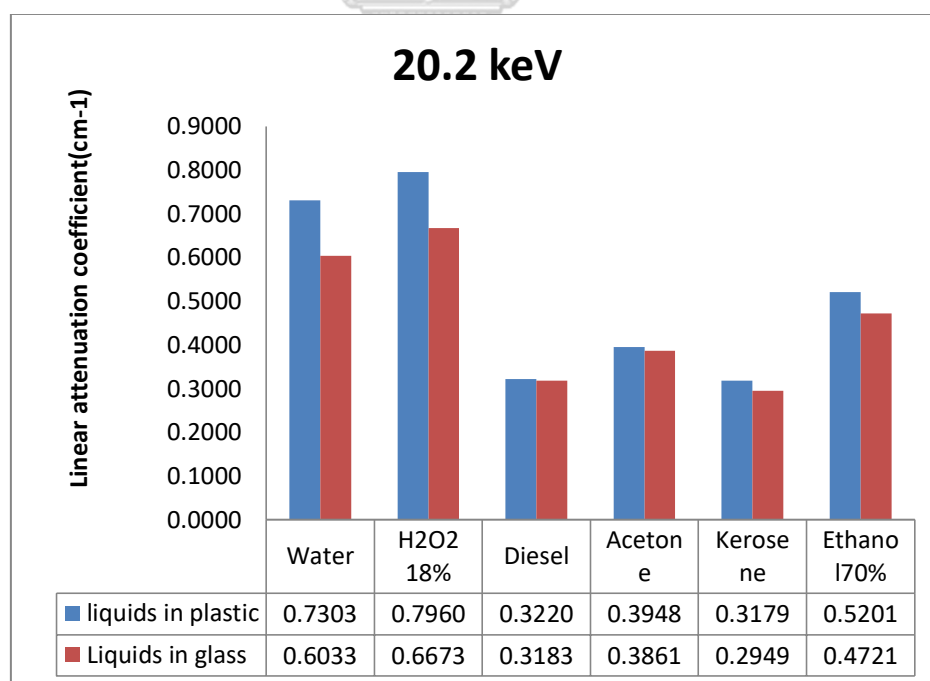
Figure 4.9 The linear attenuation of liquids in glass and plastic bottles at 20.2 keV.

43.5 keV

	Water	H2O2 18%	Diesel	Acetone	Kerosene	Ethanol70%
Liquids in plastic	0.2371	0.2666	0.1720	0.1797	0.1817	0.2043
Liquids in glass	0.2222	0.2576	0.1649	0.1555	0.1551	0.1819
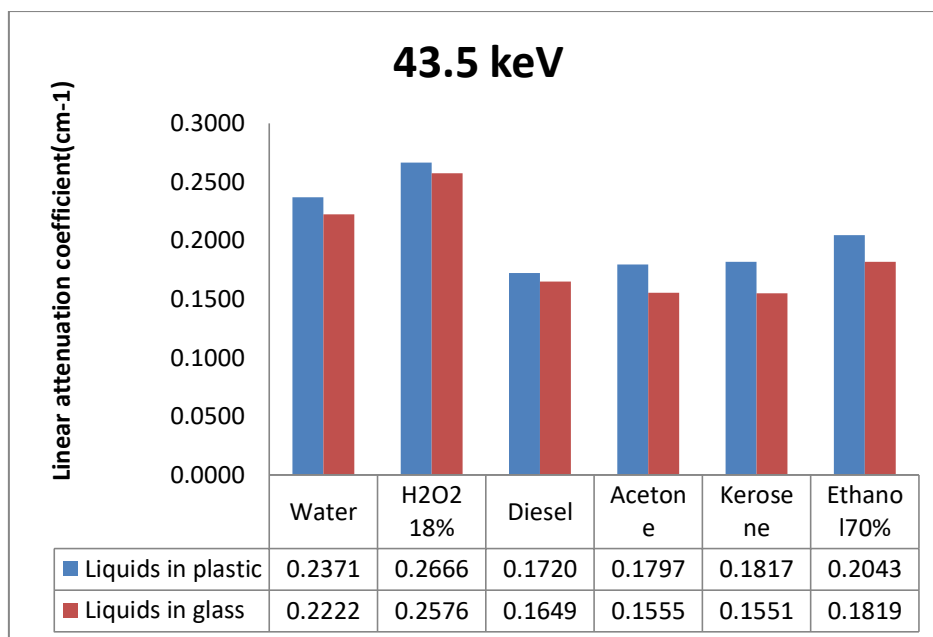
Figure 4.10 The linear attenuation of liquids in glass and plastic bottles at 43.5 keV.

Most of the cans are fully filled with liquids, so the thickness of aluminum and steel cans must be estimated from the obtained linear attenuation coefficient of cans and the thickness of 0.01 cm for aluminum and 0.02 for steel cans.

Some kinds of liquids contained in metal cans were tested for determination of the linear attenuation coefficients including water, soft drink, hydrogen peroxide, coffee, milk, diesel oil, acetone, alcohol, and kerosene. The results are shown in Table 4.29.

Table 4.29 Average linear attenuation coefficients (cm^{-1}) of liquids contained in metal cans

Type of liquids	Average linear attenuation coefficient (cm^{-1})			
	13.6 keV	17.2 keV	20.1 keV	43.5 keV
Softdrink	I_x is too low for calculation	1.1310±0.0094	0.7356±0.0027	0.2362±0.0081
Water		1.1036±0.0046	0.7206±0.0030	0.2295±0.0046
H$_2$O$_2$(12%)		1.1769±0.0055	0.7626±0.0034	0.2392±0.0047
Nescafe(coffee)		I_x is too low for calculation		0.2380±0.0091
Carabao(coffee)				0.2302±0.0090
Birdy(coffee)				0.2291±0.0107

Table 4.29(continue) Average linear attenuation coefficients (cm^{-1}) of liquids contained in metal cans

Type of liquids	Average linear attenuation coefficient (cm^{-1})			
	13.6 keV	17.2 keV	20.1 keV	43.5 keV
Milk	I_x is too low for calculation			0.2365±0.0064
Diesel	0.7442±0.0027	0.4428±0.0008	0.3214±0.0011	0.1778±0.0042
Acetone	1.0141±0.0055	0.5603±0.0011	0.3866±0.0013	0.1802±0.0042
Ethanol70%	1.5598±0.0231	0.7649±0.0019	0.5084±0.0018	0.2045±0.0044
Kerosene	0.6979±0.0024	0.4170±0.0008	0.3032±0.0011	0.1632±0.0041

The results show that linear attenuation coefficients of liquids in cans had the same trend from plastic and glass bottle. Steel cans have high linear attenuation coefficient so that transmitted intensity (I_x) was too low to calculate at low energy (13.6-20.1 keV). The linear attenuation coefficients of coffee and milk in steel cans could be determined using the 43.5 keV gamma-ray peak.

There are two types of can including aluminum cans and steel cans. The average linear attenuation coefficient of aluminum cans at 20.1 keV is 9.6949±0.4472 cm^{-1} while that of steel cans is as high as 145.2940±2.7782 cm^{-1}. Nevertheless, the thickness of aluminum and steel cans were found to be about the same at 0.01 cm and 0.02 cm respectively. Thus, attenuation correction of x-rays by aluminum and steel cans can be easily calculated by using the obtained linear attenuation coefficients and these thicknesses.

4.4.2 Result of bottle without air gap inside

Commercial liquid contained in cans were tested including drinking water, orange juice, milk, green tea, and coffee. The estimated thickness of PET plastic, HDPE plastic, aluminum can and steel can were 0.02, 0.05, 0.01 and 0.02 cm respectively whereas thickness of glass bottle were be obtained by ultrasonic thickness gauge. The results are shown in the tables below.

Table 4.30 The calculated I_0 obtained from the estimated thickness of the plastic bottles

	Estimate thickness (cm) (2 sides)	Intensity at each energy			
		13.6 keV	17.2 keV	20.1 keV	43.5 keV
I_{air}	-	184615	324206	83434	2959
I_0 HDPE$_{milk}$	0.1	165566	307369	80341	2959*
I_0 PET	0.04	168144	309352	81718	2959*
I_0 HDPE$_{Shampoo}$	0.1	157003	296883	79477	2959*
I_0 Can	0.02	99465	237575	68027	2898

*μ of plastic at 43.5 keV is very low thus I_0 is approximately I_{air}

Table 4.31 The calculated I_0 obtained from the estimated thickness of the glass bottles

	Estimate thickness (cm) (2 sides)	Intensity at each energy			
		13.6 keV	17.2 keV	20.1 keV	43.5 keV
I_0 Soy milk Glass	0.400 (UT)	I_x is too low for calculation	4468	7760	3607
I_0 Beer Glass	0.538 (UT)		803	2704	3102
I_0 Orange Juice Glass	0.350 (UT)		8319	11370	3810

Table 4.32 The calculated I_0 obtained from the estimated thickness of different types of bottles

Liquids	Diameter (cm)	Intensity at each energy			
		13.6 keV	17.2 keV	20.1 keV	43.5 keV
HDPE (Milk)	5.20	0	636	1414	828
PET (Coco)	5.10	0	1058	2001	839
PET (Green tea)	4.70	24	1160	2112	835
PET (Cocomix)	4.7	0	1459	2470	958

Table 4.32(continue) The calculated I_0 obtained from the estimated thickness of different types of bottles

Liquids	Diameter (cm)	Intensity at each energy			
		13.6 keV	17.2 keV	20.1 keV	43.5 keV
PET (Orange juice)	5.00	2	644	1379	751
PET (Soft drink)	5.65	5	614	1406	773
HDPE (Shower cream)	4.15	13	1005	1961	895
Can (Soft drink)	5.30	4	755	1503	722
Can (Beer)	6.60	21	228	663	662
Glass (Soy milk)	5.98	0	636	1414	828
Glass (Beer)	5.90	0	1058	2001	839
Glass (Orange juice)	5.67	24	1160	2112	835

From table 4.31 and 4.32, the linear attenuation coefficients of liquids in commercial bottles were calculated and presented in table 4.33.

Table 4.33 The linear attenuation coefficients of liquids in different types of bottles

Liquids	Diameter (cm)	Linear attenuation coefficient of liquids (cm^{-1})			
		13.6 keV	17.2 keV	20.1 keV	43.5 keV
HDPE (Milk)	5.20	I_x is too low for calcula-tion	1.2119±0.0078	0.7921±0.0053	0.2497±0.0077
PET (Coco)	5.10		1.1222±0.0061	0.7331±0.0045	0.2491±0.0077
PET (Green tea)	4.70		1.1987±0.0063	0.7845±0.0047	0.2715±0.0084
PET (Cocomix)	4.70		1.1495±0.0056	0.7509±0.0044	0.2420±0.0080
PET (Orange juice)	5.00		1.2449±0.0080	0.8230±0.0055	0.2765±00082
PET (Soft drink)	5.65		1.1091±0.0072	0.7242±0.0048	0.2393±0.0072

Table 4.33(continue) The linear attenuation coefficients of liquids in different types of bottles

Liquids	Diameter (cm)	Linear attenuation coefficient of liquids (cm^{-1})			
		13.6 keV	17.2 keV	20.1 keV	43.5 keV
HDPE (Shower cream)	4.15		1.4045±0.0078	0.9141±0.0056	0.2953±0.0094
Can (Soft drink)	5.30		1.0872±0.0069	0.7207±0.0049	0.2627±0.0079
Can (Beer)	6.60	I_x is too low for calcula-tion	1.0545±0.0101	0.7027±0.0059	0.2241±0.0065
Glass (Soy milk)	5.98		I_x is too low for calculation	I_x is too low for calculation	0.2343±0.0902
Glass (Beer)	5.90				0.2322±0.0706
Glass (Orange juice)	5.67				0.2484±0.1009

The results show that liquids in commercial bottles can be classified by using low energy x-ray transmission technique. Most of the commercial bottles have diameter ranging about 4-6 cm, so x-ray energy 13.6 keV cannot penetrate through the bottle and liquid. The appropriate x-ray energy in this technique is 17.2 keV but when the bottle diameter higher, the higher x-ray energy can be used.
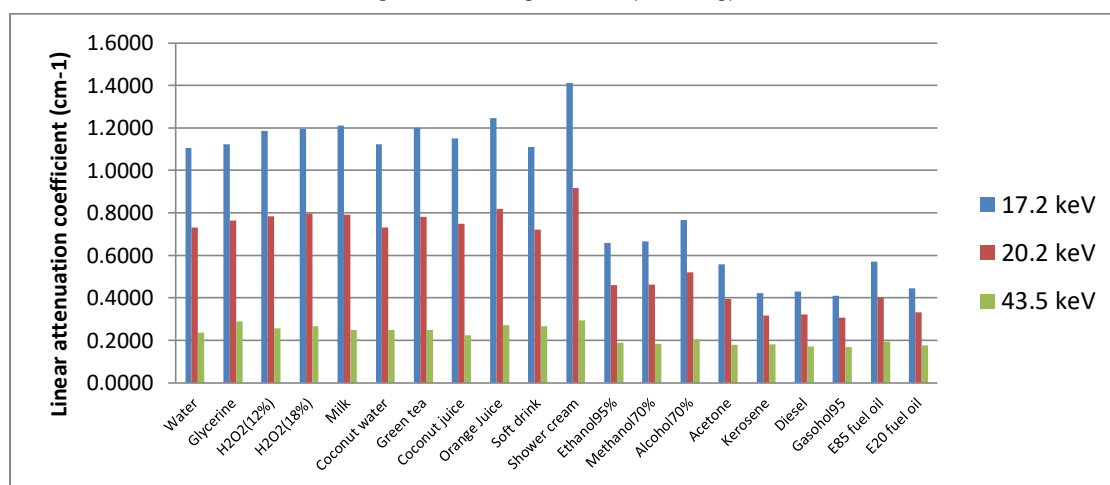
Figure 4.11 Linear attenuation coefficient of liquids at each energy.

Table 4.34 Summary of the linear attenuation coefficients of liquids at each energy

Liquids	Linear attenuation coefficient (cm^{-1}) at each energy (keV)			
	13.6 keV	17.2 keV	20.2 keV	43.5 keV
Water		1.1046	0.7303	0.2371
Glycerine		1.1233	0.7636	0.2891
H_2O_2 (12%)		1.1864	0.7844	0.2563
H_2O_2 (18%)		1.1955	0.7960	0.2666
Milk	I_x is too low for calculation	1.2098	0.7924	0.2497
Coconut water		1.1233	0.7300	0.2491
Green tea		1.2000	0.7811	0.2500
Coconut juice		1.1508	0.7475	0.2229
Orange Juice		1.2461	0.8198	0.2710
Soft drink		1.1102	0.7213	0.2653
Shower cream		1.4105	0.9170	0.2953
Ethanol 95%	1.2112	0.6588	0.4596	0.1892
Methanol 70%	1.2389	0.6666	0.4613	0.1844
Alcohol 70%	1.4365	0.7664	0.5201	0.2043
Acetone	1.0255	0.5570	0.3948	0.1797
Kerosene	0.7154	0.4230	0.3179	0.1817
Diesel	0.7395	0.4296	0.3220	0.1720
Gasohol 95	0.7036	0.4106	0.3064	0.1675
E85 fuel oil	1.0279	0.5695	0.4012	0.1932
E20 fuel oil	0.7793	0.4448	0.3308	0.1762
Benzene 95	0.6600	0.3900	0.2800	0.1500

Discussion

The x-ray energy that suitable for low energy x-ray transmission technique is depending on the bottle diameter. The 13.6 keV x-ray give excellent results to distinguish kind of liquid but its penetrating power is limited to about 3 cm. Multi-energy source like ^{238}Pu is very useful for larger diameter bottles because 17.6 keV and 20.1 keV x-rays as well as 43.5 keV gamma-ray can be utilized. But the intensity of the 20.1 keV-x-ray and the 43.5 keV-gamma-ray are too low for short counting time. For a larger bottle, ^{238}Pu may be replaced by ^{241}Am source which emits Np L x-rays nearly the same energies as those of ^{238}Pu as can be seen in table 2.1. Very importantly, the source window has to be made of thin beryllium (Be) window to allow Np L x-rays to come out. Moreover, ^{241}Am also emits 59.5 keV gamma-ray at much higher percentage (~36%) and 26.3 keV gamma-ray (2.5%) in comparison to 43.5 keV (~0.4%) of ^{238}Pu. The source activity is a major factor that affect the counting time. Only about 10 mCi or 0.37 GBq ^{238}Pu is used in this research which seems to be very low. The activity should be increased to 100 mCi (3.7 GBq) or more to shorten the counting time.

The detector is another important factor. The 5 mm x 5 mm CdTe detector used in this experiment is very small but it gives very good energy resolution with relatively low detection efficiency. All major peaks can be observed separately. Larger CdTe detectors are now available for higher detection efficiency. A low energy high purity germanium detector with Be window gives much higher detection efficiency with better energy resolution But its size, cooling system and cost may not be appropriate for a compact system. A gas proportional detector may be another choice of detector. It gives poorer energy resolution but may be enough for this purpose. All three energy peaks from ^{238}Pu x-rays are not completely resolved. Integration of all three peaks together may be applicable for this purpose. The only drawback is its detector efficiency drops rapidly beyond about 30 keV.

It will be better to have two sets of source-detector for inspection the bottle at 2 positions such as at the liquid portion and at the empty portion.

For fixed liquid thickness at 4.5 cm, uncertainty of the measurement is caused by curvature of the container as shown in figure 4.12 and figure 4.13. This error can be solved by applying a correction factor which can be obtained from experiment or calculation. If the x-ray beam is narrower, this error should be reduced.
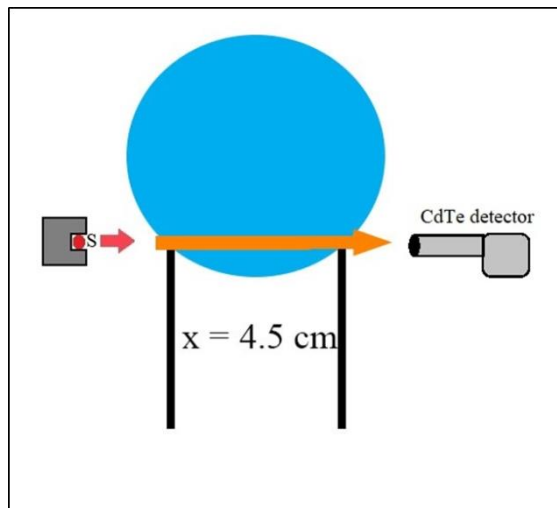
Figure 4.12 Photon through the liquid for a large bottle diameter.
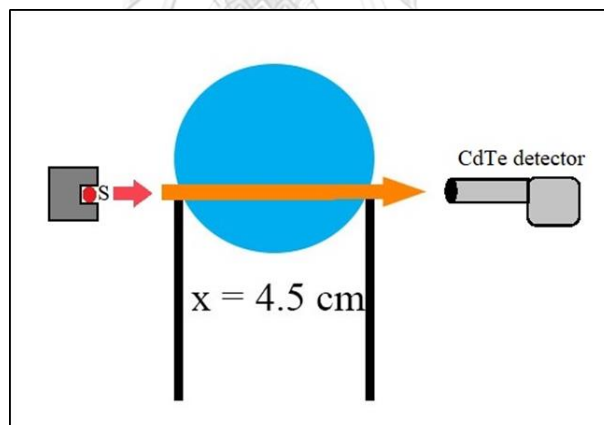
Figure 4.13 Photon through the liquid for a small bottle diameter.

Thickness of the plastic bottle can be estimated due to linear attenuation coefficient of plastic is very low. In contrast with glass and can, the linear attenuation coefficient of glass and can are very high but can is a thin bottle and the thickness of can is the same all of the bottle so that the thickness of can may be estimated by 0.01 cm for aluminum and 0.02 cm for steel can.

The thickness of glass bottle is not the same at different position due to its production process. Estimation of thickness can cause large error. The thickness of glass has to be measured by the ultrasonic thickness gauge at the same position with the x-ray transmission technique.

Conceptual design of the prototype equipment to be used for screening of liquid in unopened bottles at airports is shown in Figure 4.14 and Figure 4.15.
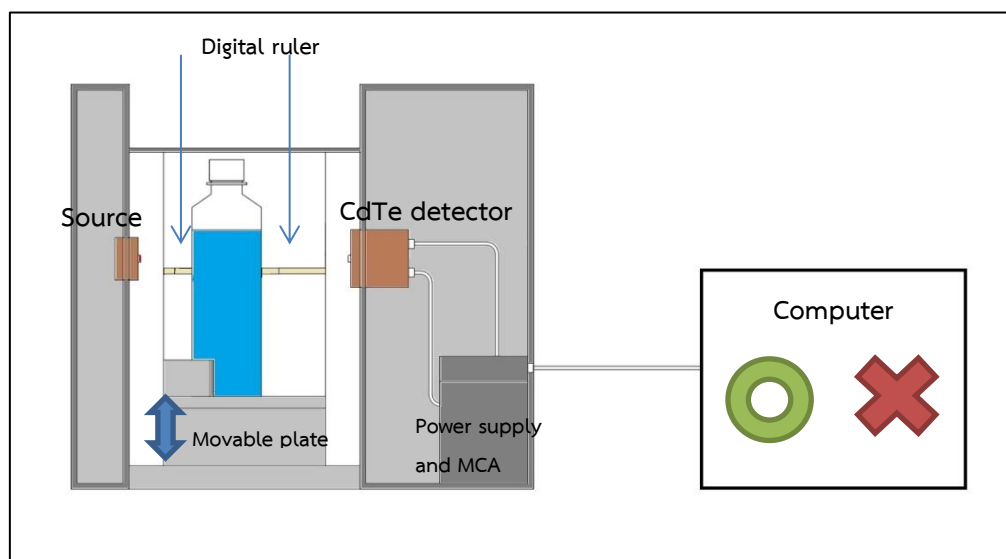
Figure 4. 14 Diagram of the prototype equipment to be used for screening of liquid in unopened bottle at airports (Side view)
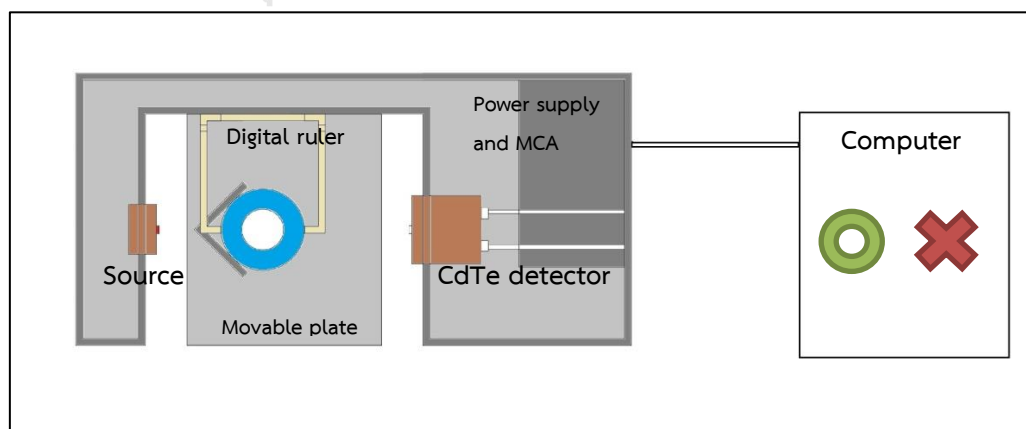
Figure 4.15 Diagram of the prototype equipment to be used for screening of liquid in unopened bottle at airports (Top view)

Radioisotope source and detector are positioned on the opposite side of the bottle under inspection. The movable plate at the bottom can be moved up and down to measure incident and transmitted intensity at a desired position. The bottle diameter is measured by a digital ruler that installed behind the bottle under inspection. The bottle can be centered by the angle plate that mounted with the movable plate at the bottom. The detector is connected to a power supply and a digital spectrum analyzer which is connected to a computer to display spectrum, perform spectrum analysis, report analysis results and any other functions to assist the operator. A data base system for bottle type, linear attenuation coefficients of liquids, bottle thickness and materials are included in the computer system.

CHAPTER V

CONCLUSION

The proposed technique is simple but can distinguish kinds of liquid efficiently. The separation factors between different kinds of liquid are very high. The technique can even distinguish differences in concentration of the same substance such as percentage of ethanol, kinds of fuel oil, etc. For example, the linear attenuation coefficients of benzene 95, gasohol 95 (10% ethanol), gasohol E20 (20% ethanol), gasohol E85 (85% ethanol) and ethanol (95%) at 13.6 keV x-rays are about 0.6660, 0.7036, 0.7793, 1.0279 and 1.2112 cm^{-1} respectively. These increases in the linear attenuation coefficients are caused by increase in percentage of ethanol from 0 to 95 %. The multiple x-rays energy gives choices to select appropriate energy peaks to be used for screening in single measurement. The only thing that still needs further investigation is to collect data related to bottle and bottled liquid. Bottle types, bottle material and bottle thickness are different from country to country. In addition, information on bottled liquids, deleterious liquid and liquid explosive are also of great importance for screening.

In this research, the bottles are divided into 3 groups i.e. plastic bottles, glass bottles and metal cans. Plastic bottles are made of PET, PE and HDPE whose linear attenuation coefficients are not high and are in the same range as liquid. PET bottles are thin such as water, soft drink and fruit juice bottles are about 0.01 – 0.02 cm thick. PE or HDPE bottles such as milk, dairy products, fruit juice are about 0.04 – 0.07 cm thick. Measurement of I_0 is preferable when there is air portion in transparent bottles. For opaque bottle like HDPE and PE, scanning for air portion is actually possible but it will take time. Thus, the average linear attenuation coefficient of the HDPE bottles is used together with the estimated thickness to calculate I_0. This method is also applied for aluminum and steel cans. For glass bottles, the average linear attenuation coefficient of glass bottles is used together with the bottle thickness measured by the ultrasonic thickness gauge. However,

transparent bottles (such as beer, wine and fruit juice) can actually be measured by x-ray transmission at the air portion but non-uniform thickness of glass may cause large error.

Table 5.1 Conclusion of procedure for determining the linear attenuation coefficients of bottled liquid

Bottle type	Method to obtain I_0
Plastic - PET (with air portion) - PET (without air portion) - HDPE (opaque)	 - X-ray transmission at the air portion - Calculated from μ and the estimated bottle thickness of 0.02 cm - Calculated from μ and the estimated bottle thickness 0.05 cm
Glass - Glass (with air portion) - Glass (without air portion)	 - X-ray transmission at the air portion - Calculated from μ and the bottle thickness obtained from ultrasonic thickness gauge
Metal Cans - Aluminum (opaque) - Steel (opaque)	 - Calculated from μ and the estimated bottle thickness of 0.01 cm - Calculated from μ and the estimated bottle thickness of 0.02 cm

The equipment for use in liquid screening at airports should be compact, easy to operate and reliable. Sensitivity of the proposed technique is obviously good but to bring it to routine inspection is still a big challenge. A data base of bottle types and liquids should be carefully developed to assist in screening the bottled liquid. Further investigation related to bottle type and bottled liquids should be conducted to collect more information to be used in screening of unwanted and deleterious liquids.

REFERENCES

1. Q&A: Liquid explosives [Internet]. 2006 [cited 19 January 2014]. Available from: http://news.bbc.co.uk/2/hi/science/nature/4780391.stm.

2. Liquids, aerosols and gels [Internet]. [cited 29 November 2016]. Available from: https://ec.europa.eu/transport/modes/air/security/aviation-security-policy/lags_en.

3. Gonga Q, Stoianb R-I, Coccarellia DS, Greenberga JA, Verac E, Gehma ME. Rapid simulation of X-ray transmission imaging for baggage inspection via GPU-based ray tracing. Nucl Instrum Methods Phys Res B. 2018;415:100-9.

4. Harding G. X-ray scatter tomography for explosives detection. Radiat Phys Chem. 2004;71:869-81.

5. Gudmundson E, Jakobsson A, Poplett I, Smith J, editors. Detection and Classification of Liquid Explosives Using NMR. IEEE International Conference on Acoustics, Speech, and Signal Processing; 2009; Taipei Taiwan.

6. Eliasson C, Macleod NA, Matousek P. Noninvasive detection of concealed liquid explosive using Raman spectroscopy. Anal Chem. 2007;79:8185-9.

7. Liquid Explosives Detection in Transparent Containers [Internet]. 2010 [cited 17 January 2017]. Available from: http://www.laser-detect.com/brochures/Liquids.pdf.

8. Kuznetsov AV, Osetrov OI, editors. Overview of Liquid Explosives' Detection. NATO Advanced Research Workshop on Detection of Liquid Explosives and Flammable Agents in Connection with Terrorism; 2007; St. Petersburg, Russia: Springer.

9. Wells K, Bradley D. A review of X-ray explosives detection techniques for checked baggage. Appl Radiat Isot. 2012;70(8):1729–46.

10. Matyas R, Chylkova J. Study of TATP: Method for determination of residual acids in TATP. Forensic Sci Int. 2013;228:170-3.

11.   Oxley JC, editor What's Special About Liquid Explosives? NATO Advanced Research Workshop on Detection of Liquid Explosives and Flammable Agents in Connection with Terrorism; 2007; St. Petersburg, Russia: Springer.

12.   Dongarge SM, Mitkar SR. Measurement of linear and mass attenuation coefficient of alcohol soluable compound for γ-rays at energy 0.36 MeV. J Chem Pharm Res. 2012;4(6):3116-20.

13.   Midgley S. Measurements of the X-ray linear attenuation coefficient for low atomic number materials at energies 32-66 and 140 keV. Radiat Phys Chem. 2005;72:525-35.

14.   Gupta M, Sidhu B, Mann K, Dhaliwal A, Kahlon K. Advanced two media (ATM) method for measurement of linear attenuation coefficient. Ann Nucl Energy. 2013;56:251-4.

15.   Nelson G, Reilly D. Gamma-Ray Interactions with Matter. Washington DC, USA: Los Alamos National Laboratory; 1991. 27-38 p.

16.   Introdution to non-destructive testing techniques [Internet]. [cited 3 Apirl 2017]. Available from: https://eis.hu.edu.jo/ACUploads/10526/Ultrasonic%20Testing.pdf.

17.   Knoll GF. Radiation Detection and Measurement. edition t, editor. New York: John Wley & Sons; 2000.

18.   Choppin G, Ryberg J. Nuclear Chemistry: Theory and Applications. New York: Pergamon; 1980.

19.   Potts PJ. Handbook of Silicate Rocks Analysis. New York: Springer; 1992.

20.   Redus B. Efficiency and Atennuation in CdTe Detectors. Amptek Inc.: Amptek Application Note AN-CdTe-001; 2010.

21.   X-ray and gamma ray detector high resolution CdTe cadmium telluride [Internet]. amptek. [cited 20 September 2017]. Available from: http://www.amptek.com/pdf/xr100cdte.pdf.

22.   The Different Types Of Plastics And Their Classifications [Internet]. 2016 [cited 16 December 2016]. Available from: https://www.linkedin.com/pulse/different-types-plastics-classifications-jane-huang.

23. Piller R. 2016. [cited 2016]. Available from: http://blog.ecomarketingsolutions.com/tag/recycling-symbols.

24. The status of Flat Soda Lime Silicate Glass and its raw materials under REACH [Internet]. (Regulation (EC) No 1907 /2006)-REACH. 2016 [cited 4 March 2017]. Available from: http://www.glassforeurope.com/images/cont/167_32370_file.pdf.

25. Types of can [Internet]. n.d. [cited 5 March 2017]. Available from: https://www.toyo-seikan.co.jp/e/technique/can/kind/.

APPENDIX

I.) Incident intensity(I_0), transmitted intensity(I_X) and linear attenuation coefficient of liquids in effect of bottle diameter.

Drinking Water

Bottle diameter (cm.)	Liquid thickness (cm.)	Intensity I_0 at each energy (120seconds)				
		13.6 keV	17.2 keV	20.1 keV	60 keV	122 keV
2.26	1.96	109627	243863	62009	130551	19761
3.10	2.98	129487	261265	63812	135346	20089
3.33	3.17	118884	249557	62622	134134	19844
3.82	3.62	121748	253346	62280	134545	20187
4.96	4.84	125269	256144	62098	134970	20169
7.40	7.32	104689	217219	56621	136518	20503

Bottle diameter (cm.)	Liquid thickness (cm.)	Intensity I_X of water at each energy (120seconds)				
		13.6 keV	17.2 keV	20.1 keV	60 keV	122 keV
2.26	1.96	1570	25095	14318	88225	14122
3.10	2.98	274	9548	7673	74628	12305
3.33	3.17	123	6804	6278	70823	12312
3.82	3.62	73	4286	4467	64793	11336
4.96	4.84	10	1138	1845	51625	9354
7.40	7.32	6	102	340	25293	5304

Bottle diameter (cm.)	Liquid thickness (cm.)	Linear attenuation coefficient of water (cm^{-1})				
		13.6 keV	17.2 keV	20.1 keV	60 keV	122 keV
2.26	1.96	2.1663	1.1602	0.7478	0.1999	0.1714
3.10	2.98	2.0665	1.1105	0.7108	0.1998	0.1645

3.33	3.17	2.1684	1.1363	0.7256	0.2015	0.1506
3.82	3.62	2.0495	1.1269	0.7279	0.2019	0.1594
4.96	4.84	I_X is low to	1.1191	0.7265	0.1986	0.1587
7.40	7.32	calculate	1.0470	0.6988	0.2303	0.1847
Average LAC		2.1127 ±0.0635	1.1167 ±0.0382	0.7229 ±0.0167	0.2053 ±0.0123	0.1649 ±0.0119

Beer

Bottle diameter (cm.)	Liquid thickness (cm.)	Intensity I_0 at each energy (120seconds)				
		13.6 keV	17.2 keV	20.1 keV	60 keV	122 keV
2.26	1.96	109627	243863	62009	130551	19761
3.10	2.98	129487	261265	63812	135346	20089
3.33	3.17	118884	249557	62622	134134	19844
3.82	3.62	121748	253346	62280	134545	20187
4.96	4.84	125269	256144	62098	134970	20169
7.40	7.32	104689	217219	56621	136518	20503

Bottle diameter (cm.)	Liquid thickness (cm.)	Intensity I_X of beer at each energy (120seconds)				
		13.6 keV	17.2 keV	20.1 keV	60 keV	122 keV
2.26	1.96	1136	19662	12015	87070	14358
3.10	2.98	242	8958	7184	73435	12131
3.33	3.17	166	7092	6307	70142	11807
3.82	3.62	51	4166	4429	64000	11027
4.96	4.84	5	1139	1896	50875	9357
7.40	7.32	9	57	293	24840	5192

Bottle diameter	Liquid thickness	Linear attenuation coefficient of beer (cm^{-1})				
		13.6 keV	17.2 keV	20.1 keV	60 keV	122 keV

(cm.)	(cm.)					
2.26	1.96	2.3314	1.2847	0.8373	0.2067	0.1630
3.10	2.98	2.1082	1.1319	0.7329	0.2052	0.1693
3.33	3.17	2.0738	1.1233	0.7241	0.2045	0.1638
3.82	3.62	2.1486	1.1348	0.7302	0.2053	0.1670
4.96	4.84	I_X is low to	1.1189	0.7209	0.2016	0.1587
7.40	7.32	calculate	1.1264	0.7191	0.1952	0.1573
Average LAC		2.1655 ±0.1148	1.1533 ±0.0646	0.7441 ±0.0460	0.2031 ±0.0042	0.1632 ±0.0046

Soft drink

Bottle diameter (cm.)	Liquid thickness (cm.)	Intensity I_0 at each energy (120seconds)				
		13.6 keV	17.2 keV	20.1 keV	60 keV	122 keV
2.26	1.96	109627	243863	62009	130551	19761
3.10	2.98	129487	261265	63812	135346	20089
3.33	3.17	118884	249557	62622	134134	19844
3.82	3.62	121748	253346	62280	134545	20187
4.96	4.84	125269	256144	62098	134970	20169
7.40	7.32	104689	217219	56621	136518	20503

Bottle diameter (cm.)	Liquid thickness (cm.)	Intensity I_X of soft drink at each energy (120seconds)				
		13.6 keV	17.2 keV	20.1 keV	60 keV	122 keV
2.26	1.96	1386	22662	12818	85722	14370
3.10	2.98	186	8022	6664	71867	12288
3.33	3.17	155	6204	5318	68442	11760
3.82	3.62	42	3611	3943	62595	11065
4.96	4.84	18	1003	1670	49678	8893
7.40	7.32	5	27	118	23158	5110

Bottle diameter (cm.)	Liquid thickness (cm.)	Linear attenuation coefficient of soft drink (cm^{-1})				
		13.6 keV	17.2 keV	20.1 keV	60 keV	122 keV
2.26	1.96	2.2299	1.2122	0.8043	0.2146	0.1625
3.10	2.98	2.1965	1.1689	0.7581	0.2124	0.1649
3.33	3.17	2.0954	1.1655	0.7779	0.2123	0.1650
3.82	3.62	2.2022	1.1742	0.7623	0.2114	0.1661
4.96	4.84	I_X is low to calculate	1.1452	0.7471	0.2065	0.1692
7.40	7.32		1.0301	0.7072	0.2032	0.1591
Average LAC		**2.1810 ±0.0589**	**1.1494 ±0.0624**	**0.7595 ±0.0324**	**0.2101 ±0.0043**	**0.1645 ±0.0034**

Ethanol(70%)

Bottle diameter (cm.)	Liquid thickness (cm.)	Intensity I_0 at each energy (120seconds)				
		13.6 keV	17.2 keV	20.1 keV	60 keV	122 keV
2.26	1.96	109627	243863	62009	130551	19761
3.10	2.98	129487	261265	63812	135346	20089
3.33	3.17	118884	249557	62622	134134	19844
3.82	3.62	121748	253346	62280	134545	20187
4.96	4.84	125269	256144	62098	134970	20169
7.40	7.32	104689	217219	56621	136518	20503

Bottle diameter (cm.)	Liquid thickness (cm.)	Intensity I_X of ethanol(70%)at each energy (120seconds)				
		13.6 keV	17.2 keV	20.1 keV	60 keV	122 keV
2.26	1.96	6176	49917	20992	92942	14884
3.10	2.98	1717	24248	13119	80692	13217
3.33	3.17	1226	20272	11401	77421	12967
3.82	3.62	589	14238	8851	71408	11977

4.96	4.84	114	5065	4489	58505	9970
7.40	7.32	20	656	1149	31660	6135

Bottle diameter (cm.)	Liquid thickness (cm.)	Linear attenuation coefficient of ethanol(70%) (cm^{-1})				
		13.6 keV	17.2 keV	20.1 keV	60 keV	122 keV
2.26	1.96	1.4676	0.8093	0.5526	0.1734	0.1446
3.10	2.98	1.4507	0.7977	0.5308	0.1736	0.1405
3.33	3.17	1.4430	0.7919	0.5374	0.1734	0.1342
3.82	3.62	1.4727	0.7953	0.5390	0.1750	0.1442
4.96	4.84	1.4467	0.8106	0.5428	0.1727	0.1456
7.40	7.32	Ix low to cal.	0.7927	0.5324	0.1674	0.1382
Average LAC		**1.4561** **±0.0132**	**0.7996** **±0..0083**	**0.5392** **±0.0079**	**0.1726** **±0.0026**	**0.1412** **±0.0044**

Kerosene

Bottle diameter (cm.)	Liquid thickness (cm.)	Intensity I_0 at each energy (120seconds)				
		13.6 keV	17.2 keV	20.1 keV	60 keV	122 keV
2.26	1.96	109627	243863	62009	130551	19761
3.10	2.98	129487	261265	63812	135346	20089
3.33	3.17	118884	249557	62622	134134	19844
3.82	3.62	121748	253346	62280	134545	20187
4.96	4.84	125269	256144	62098	134970	20169
7.40	7.32	104689	217219	56621	136518	20503

Bottle diameter (cm.)	Liquid thickness (cm.)	Intensity I_X of kerosene at each energy (120seconds)				
		13.6 keV	17.2 keV	20.1 keV	60 keV	122 keV
2.26	1.96	26405	100505	31419	97478	15286

3.10	2.98	15704	72800	24525	86056	13792
3.33	3.17	12781	63225	22238	82920	13419
3.82	3.62	9321	52566	19208	77867	12713
4.96	4.84	3945	32563	13437	65336	11026
7.40	7.32	483	8643	5130	39130	7322

Bottle diameter (cm.)	Liquid thickness (cm.)	Linear attenuation coefficient of kerosene (cm^{-1})				
		13.6 keV	17.2 keV	20.1 keV	60 keV	122 keV
2.26	1.96	0.7263	0.4522	0.3469	0.1490	0.1310
3.10	2.98	0.7079	0.4288	0.3209	0.1520	0.1262
3.33	3.17	0.7035	0.4331	0.3266	0.1517	0.1234
3.82	3.62	0.7099	0.4344	0.3249	0.1511	0.1277
4.96	4.84	0.7145	0.4261	0.3163	0.1499	0.1248
7.40	7.32	0.7348	0.4405	0.3280	0.1431	0.1179
Average LAC		**0.7161 ±0.0120**	**0.4359 ±0.0094**	**0.3273 ±0.0150**	**0.1495 ±0.0033**	**0.1252 ±0.0044**

Diesel

Bottle diameter (cm.)	Liquid thickness (cm.)	Intensity I_0 at each energy (120seconds)				
		13.6 keV	17.2 keV	20.1 keV	60 keV	122 keV
2.26	1.96	109627	243863	62009	130551	19761
3.10	2.98	129487	261265	63812	135346	20089
3.33	3.17	118884	249557	62622	134134	19844
3.82	3.62	121748	253346	62280	134545	20187
4.96	4.84	125269	256144	62098	134970	20169
7.40	7.32	104689	217219	56621	134867	20034

Bottle diameter (cm.)	Liquid thickness (cm.)	Intensity I_X of diesel at each energy (120seconds)				
		13.6 keV	17.2 keV	20.1 keV	60 keV	122 keV
2.26	1.96	23915	97021	31235	95183	14712
3.10	2.98	13335	68620	23791	82803	13243
3.33	3.17	11101	61072	22660	80407	12859
3.82	3.62	7739	49262	18882	74724	12176
4.96	4.84	3230	29850	13013	63193	10536
7.40	7.32	543	9800	5811	43315	7579

Bottle diameter (cm.)	Liquid thickness (cm.)	Linear attenuation coefficient of diesel (cm^{-1})				
		13.6 keV	17.2 keV	20.1 keV	60 keV	122 keV
2.26	1.96	0.7768	0.4702	0.3499	0.1612	0.1505
3.10	2.98	0.7628	0.4486	0.3311	0.1649	0.1398
3.33	3.17	0.7480	0.4440	0.3207	0.1614	0.1369
3.82	3.62	0.7612	0.4524	0.3297	0.1625	0.1397
4.96	4.84	0.7558	0.4441	0.3229	0.1568	0.1342
7.40	7.32	0.7188	0.4233	0.3110	0.1552	0.1328
Average LAC		0.7539 ±0.0196	0.4471 ±0.0152	0.3275 ±0.0131	0.1603 ±0.0036	0.1390 ±0.0063

Bensene95

Bottle diameter (cm.)	Liquid thickness (cm.)	Intensity I_0 at each energy (120seconds)				
		13.6 keV	17.2 keV	20.1 keV	60 keV	122 keV
2.26	1.96	109627	243863	62009	130551	19761
3.10	2.98	129487	261265	63812	135346	20089
3.33	3.17	118884	249557	62622	134134	19844
3.82	3.62	121748	253346	62280	134545	20187

| 4.96 | 4.84 | 125269 | 256144 | 62098 | 134970 | 20169 |
| 7.40 | 7.32 | 104689 | 217219 | 56621 | 134867 | 20034 |

Bottle diameter (cm.)	Liquid thickness (cm.)	Intensity I_x of bensene95 at each energy (120seconds)				
		13.6 keV	17.2 keV	20.1 keV	60 keV	122 keV
2.26	1.96	30133	114375	36356	98547	15382
3.10	2.98	17836	83320	28670	88074	13861
3.33	3.17	14970	73443	25537	85474	13586
3.82	3.62	10976	60877	22737	79383	12860
4.96	4.84	5329	39480	16696	69287	11307
7.40	7.32	1051	14729	7878	48736	8446

Bottle diameter (cm.)	Liquid thickness (cm.)	Linear attenuation coefficient of bensene95 (cm^{-1})				
		13.6 keV	17.2 keV	20.1 keV	60 keV	122 keV
2.26	1.96	0.6589	0.3863	0.2724	0.1435	0.1278
3.10	2.98	0.6652	0.3835	0.2685	0.1442	0.1245
3.33	3.17	0.6537	0.3859	0.2830	0.1422	0.1195
3.82	3.62	0.6647	0.3939	0.2784	0.1457	0.1246
4.96	4.84	0.6523	0.3864	0.2714	0.1378	0.1196
7.40	7.32	0.6286	0.3676	0.2694	0.1391	0.1180
Average LAC		0.6539 ±0.0135	0.3839 ±0.0087	0.2738 ±0.0057	0.1421 ±0.0031	0.1223 ±0.0039

Gasohol95

Bottle diameter (cm.)	Liquid thickness (cm.)	Intensity I_0 at each energy (120seconds)				
		13.6 keV	17.2 keV	20.1 keV	60 keV	122 keV
2.26	1.96	109627	243863	62009	146310	18340

3.10	2.98	129487	261265	63812	150728	18728
3.33	3.17	118884	249557	62622	151955	18871
3.82	3.62	121748	253346	62280	150483	18370
4.96	4.84	125269	256144	62098	151927	18560
7.40	7.32	104689	217219	56621	153575	18792

Bottle diameter (cm.)	Liquid thickness (cm.)	Intensity I_X of gasohol95 at each energy (120seconds)				
		13.6 keV	17.2 keV	20.1 keV	60 keV	122 keV
2.26	1.96	26248	106918	34810	110130	14647
3.10	2.98	15659	76903	26868	97389	13209
3.33	3.17	12578	68740	24920	94147	12787
3.82	3.62	9356	56367	21675	88423	12362
4.96	4.84	4080	34630	15055	75363	10603
7.40	7.32	674	12055	6829	51747	7721

Bottle diameter (cm.)	Liquid thickness (cm.)	Linear attenuation coefficient of gasohol95 (cm^{-1})				
		13.6 keV	17.2 keV	20.1 keV	60 keV	122 keV
2.26	1.96	0.7293	0.4207	0.2946	0.1449	0.1147
3.10	2.98	0.7089	0.4104	0.2903	0.1466	0.1172
3.33	3.17	0.7086	0.4067	0.2907	0.1510	0.1228
3.82	3.62	0.7088	0.4152	0.2916	0.1469	0.1094
4.96	4.84	0.7075	0.4134	0.2928	0.1449	0.1157
7.40	7.32	0.6893	0.3950	0.2890	0.1486	0.1215
Average LAC		0.7087 ±0.0127	0.4102 ±0.0088	0.2915 ±0.0020	0.1471 ±0.0024	0.1169 ±0.0049

GasoholE20

Bottle diameter (cm.)	Liquid thickness (cm.)	Intensity I₀ at each energy (120seconds)				
		13.6 keV	17.2 keV	20.1 keV	60 keV	122 keV
2.26	1.96	109627	243863	62009	146310	18340
3.10	2.98	129487	261265	63812	150728	18728
3.33	3.17	118884	249557	62622	151955	18871
3.82	3.62	121748	253346	62280	150483	18370
4.96	4.84	125269	256144	62098	151927	18560
7.40	7.32	104689	217219	56621	153575	18792

Bottle diameter (cm.)	Liquid thickness (cm.)	Intensity Iₓ of gasoholE20 at each energy (120seconds)				
		13.6 keV	17.2 keV	20.1 keV	60 keV	122 keV
2.26	1.96	24411	102035	33947	109044	14244
3.10	2.98	13337	71552	26168	97055	13287
3.33	3.17	10857	63309	24026	94084	13220
3.82	3.62	7595	52017	21025	89034	12044
4.96	4.84	3284	31299	14553	75106	10689
7.40	7.32	485	10001	6420	51075	7611

Bottle diameter (cm.)	Liquid thickness (cm.)	Linear attenuation coefficient of gasoholE20 (cm^{-1})				
		13.6 keV	17.2 keV	20.1 keV	60 keV	122 keV
2.26	1.96	0.7664	0.4445	0.3074	0.1500	0.1290
3.10	2.98	0.7628	0.4346	0.2991	0.1477	0.1152
3.33	3.17	0.7550	0.4327	0.3022	0.1512	0.1123
3.82	3.62	0.7664	0.4373	0.3000	0.1450	0.1166
4.96	4.84	0.7524	0.4343	0.2998	0.1456	0.1140

7.40	7.32	0.7342	0.4205	0.2974	0.1504	0.1235
Average LAC		0.7562 ±0.0122	0.4340 ±0.0078	0.3010 ±0.0035	0.1483 ±0.0026	0.1184 ±0.0064

GasoholE85

Bottle diameter (cm.)	Liquid thickness (cm.)	Intensity I_0 at each energy (120seconds)				
		13.6 keV	17.2 keV	20.1 keV	60 keV	122 keV
2.26	1.96	109627	243863	62009	146310	18340
3.10	2.98	129487	261265	63812	150728	18728
3.33	3.17	118884	249557	62622	151955	18871
3.82	3.62	121748	253346	62280	150483	18370
4.96	4.84	125269	256144	62098	151927	18560
7.40	7.32	104689	217219	56621	153575	18792

Bottle diameter (cm.)	Liquid thickness (cm.)	Intensity I_X of gasoholE85 at each energy (120seconds)				
		13.6 keV	17.2 keV	20.1 keV	60 keV	122 keV
2.26	1.96	15050	80666	29420	106247	14423
3.10	2.98	6495	50307	21232	94525	12874
3.33	3.17	5040	43437	18879	92029	12662
3.82	3.62	3317	33613	15874	85539	11996
4.96	4.84	994	17324	9994	71512	10335
7.40	7.32	109	4662	3742	48838	7380

Bottle diameter (cm.)	Liquid thickness (cm.)	Linear attenuation coefficient of gasoholE85 (cm^{-1})				
		13.6 keV	17.2 keV	20.1 keV	60 keV	122 keV
2.26	1.96	1.0131	0.5644	0.3804	0.1632	0.1226
3.10	2.98	1.0042	0.5528	0.3693	0.1566	0.1258

3.33	3.17	0.9971	0.5515	0.3783	0.1582	0.1259
3.82	3.62	0.9953	0.5580	0.3776	0.1560	0.1177
4.96	4.84	0.9993	0.5565	0.3774	0.1557	0.1210
7.40	7.32	0.9382	0.5248	0.3711	0.1565	0.1277
Average LAC		0.9912 ±0.0268	0.5513 ±0.0138	0.3757 ±0.0044	0.1577 ±0.0028	0.1234 ±0.0037

II.) Intensity and linear attenuation calculation for reference glass.

	Intensity in air for each energy (600 sec.)			
	13.6 keV	17.2 keV	20.1 keV	43.5 keV
I_{air}	577147	961530	260782	8897
	569865	964729	260867	8817
average I_{air}	**573506±5149**	**963129±2262**	**260824±60**	**8857±57**

	Intensity at each energy (600 sec.)			
	13.6 keV	17.2 keV	20.1 keV	43.5 keV
I_0Orange Juice glass	-	7667	13507	5871
	-	7545	13290	5903
	-	7548	13334	5459
Average $I_{0Orange\ Juice}$		**7587±70**	**13377±115**	**5744±248**

	Average linear attenuation coefficient (cm^{-1})			
	13.6 keV	17.2 keV	20.1 keV	43.5 keV
Orange Juice glass	-	11.9005	7.2918	1.0239
	-	11.9400	7.3317	1.0105
	-	11.9390	7.3236	1.2031
Average LAC$_{Orange\ Juice}$	-	**11.9265±0.0225**	**7.3157±0.0211**	**1.0791±0.1075**

	Intensity at each energy (600 sec.)			
	13.6 keV	17.2 keV	20.1 keV	43.5 keV
I_0Wine glass	-	8109	14435	6157
	-	7969	15233	6147
	-	8161	14105	6439
Average I_{0Wine}		8080±99	14591±580	6248±166

	Average linear attenuation coefficient (cm^{-1})			
	13.6 keV	17.2 keV	20.1 keV	43.5 keV
Wine glass	-	12.5708	7.7105	0.9950
	-	12.6163	7.5700	0.9992
	-	12.5541	7.7709	0.8781
Average LAC_{wine}	-	12.5804±0.0322	7.6848±0.1031	0.9574±0.1075

	Intensity at each energy (600 sec.)			
	13.6 keV	17.2 keV	20.1 keV	43.5 keV
I_0Mineral water glass	-	8166	14084	5902
	-	8091	14076	5884
	-	7877	14458	5982
Average $I_{0Mineral\ water}$		8045±150	14206±218	5923±52

	Average linear attenuation coefficient (cm^{-1})			
	13.6 keV	17.2 keV	20.1 keV	43.5 keV
Mineral water glass	-	12.3537	7.5613	1.0633
	-	12.3777	7.5627	1.0712
	-	12.4471	7.4934	1.0284
Average $LAC_{Mineral\ water}$	-	12.3938±0.0485	7.5391±0.0.96	1.0543±0.0228

III.) Intensity and linear attenuation calculation for reference cans.

	Intensity at each energy (600 sec.)			
	13.6 keV	17.2 keV	20.1 keV	43.5 keV
I_{air}	593394	993458	249927	8682
	595550	998886	251047	8780
	598182	997809	249006	8536
Average I_{air}	595708±2398	996717±2874	249993±1022	8666±123

	Intensity at each energy (600 sec.)			
	13.6 keV	17.2 keV	20.1 keV	43.5 keV
I_0Beer1 glass	-	1264	3604	4568
	-	1315	3814	4573
	-	1221	3755	4614
Average I_{0Beer1}		1267±47	3724±108	4585±25

	Average linear attenuation coefficient (cm^{-1})			
	13.6 keV	17.2 keV	20.1 keV	43.5 keV
Beer1 glass		12.1276	7.7080	1.1642
	-	12.0557	7.6050	1.1623
	-	12.1905	7.6334	1.1460
Average LAC_{Beer1}	-	12.1256±0.0675	7.6498±0.0532	1.1585±0.0100

	Intensity at each energy (600 sec.)			
	13.6 keV	17.2 keV	20.1 keV	43.5 keV
I_0Beer2 glass	-	2093	5675	4790
	-	2119	5685	4934
	-	1916	5855	4915
Average I_{0Beer2}		2043±110	5738±101	4880±78

	Average linear attenuation coefficient (cm^{-1})			
	13.6 keV	17.2 keV	20.1 keV	43.5 keV
Beer2 glass	-	13.0910	8.0369	1.2588
	-	13.0648	8.0331	1.1959
	-	13.2786	7.9706	1.2041
Average LAC$_{Beer2}$	**-**	**13.1458±0.1166**	**8.0145±0.0372**	**1.2206±0.0342**

	Intensity in air at each energy (600 sec.)			
	13.6 keV	17.2 keV	20.1 keV	43.5 keV
I$_{air}$	633137	1065110	266073	9973
	634536	1071476	272643	9740
average I$_{air}$	**633837±989**	**1068293±4501**	**269358±4646**	**9857±165**

Type of can	Intensity at each energy (600 sec.)			
	13.6 keV	17.2 keV	20.1 keV	43.5 keV
Green tea	339887	784614	223829	9590
	340706	787261	222918	9466
Average I$_{0Green\ tea}$	**340297±579**	**785938±1872**	**223374±644**	**9528±88**
Soft drink	345155	785750	223417	9580
	344313	788722	221929	9606
Average I$_{0Soft\ drink}$	**344734±595**	**787236±2102**	**222673±1052**	**9593±18**
Beer	340308	781053	218591	9700
	342678	784623	220648	9607
Average I$_{0Beer}$	**341493±1676**	**782838±2524**	**219620±1455**	**9654±66**

Type of can	Average linear attenuation coefficient (cm^{-1})			
	13.6 keV	17.2 keV	20.1 keV	43.5 keV
Green tea	31.1589	15.4313	9.2579	1.3705
	31.0386	15.2629	9.4619	2.0212
Average	**31.0987±0.0851**	**15.3471±0.1191**	**9.3599±0.1442**	**1.6959±0.4601**

LAC$_{Green\ tea}$				
Soft drink	30.3899	15.3589	9.3501	1.4227
	30.5120	15.1702	9.6842	1.2872
Average LAC$_{Soft\ drink}$	**30.4509±0.0864**	**15.2646±0.1335**	**9.5171±0.2363**	**1.3549±0.0958**
Beer	31.0970	15.6587	10.4419	0.8003
	30.7500	15.4307	9.9736	1.2820
Average LAC$_{Beer}$	**30.9235±0.2454**	**15.5447±0.1612**	**10.2078±0.3311**	**1.0411±0.3406**

จุฬาลงกรณ์มหาวิทยาลัย

CHULALONGKORN UNIVERSITY

VITA

Name: Parkphum Orachorn

Date of birth: 22 November 1984

Education: Bachelor of Science (Physics) Khonkaen University 2002-2005

Master of Science(Nuclear Technology) Chulalongkorn University 2006-2009

Address: 179/3 moo9 Chongsammor Kaengkhro Chaiyaphum Thailand 36150

Scholarship: Development and Promotion of Science and Technology Talents Project (DPST)